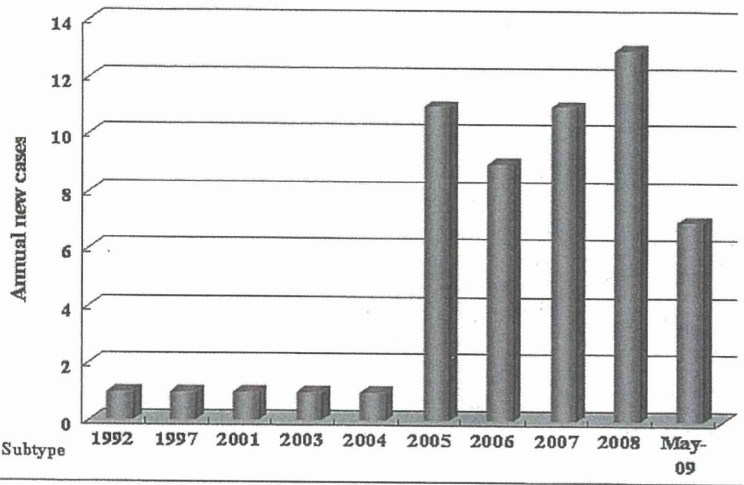

HIV-1 Subtype	1992	1997	2001	2003	2004	2005	2006	2007	2008	May-09
B (Cluster 1)						6	4	6	3	
B (Cluster 2)					1		2	2	2	1
B									2	1
C						1	1			
G									1	1
CRF01_AE								1		
CRF02_AG		1				1		2		
Unavailable	1		1	1		3	2		5	4
Total	1	1	1	1	1	11	9	11	13	7

FIG. 2. Year-diagnosis rates of HIV-1 infection in Mongolia between 1992 and May 2009 (upper panel). The number of patients and their identified HIV-1 subtypes are listed in the lower panel.

database in the Los Alamos National Laboratory with their sampling time. The reference alignment set for the *pol* region consists of 22 sequences of subtype B viruses covering Korea, China, Japan, Russia, Europe, and North America, with the sequence of D.KE.97.ML415_2 as the subtype's outgroup. The set for the *env* region consists of 20 sequences of subtype B viruses covering Korea, China, Japan, Russia, Europe, and North America, with the sequence of C.US.98US_MSC5016 as the subtype's outgroup. Each reference set was piled up with the Mongolian sequence analyzed in the present study and realigned using CLUSTAL-W. The following analyses were performed in each region of the sequence alignment. The nucleotide substitution model used in the analyses was evaluated by the hierarchical likelihood ratio test using PAUP v4.0 beta[9] with MrModel test,[10] and the general time-reversible (GTR) model[11] with both invariant sites (I) and gamma-distributed site heterogeneity (G) with four rate categories had maximum likelihood. Bayesian MCMC analyses were performed by BEAST v1.4.8[12] using the GTR+I+G and a relaxed molecular clock model (the uncorrelated lognormal-distributed model).[13] Three different population dynamic models, Exponential growth, Logistic growth, and Bayesian Skyline Plot (BSP), were tested in the analyses, and the exponential model was adopted as the most likely phylogeny according to the BSP property. Each Bayesian MCMC analysis was run for 30 million states and sampled every 10,000 states. Posterior probabilities were calculated with a burn-in of 4 million states and checked for convergence using Tracer v1.4. The maximum clade credibility tree for the analyzed set of the MCMC data was annotated by TreeAnotator in the BEAST package. The posterior distribution of the substitution rate obtained from the heterochronous sequences was subsequently incorporated as a prior distribution for evolutionary rate of the *pol* region as well as the *env* region, thereby adding a timescale to the phylogenetic histories of the given viruses and enabling the estimation of the times of the most recent common ancestors (tMRCA).[14]

Results

The *pol* region (1065 bp) was successfully amplified and sequenced in 41 sera. According to the REGA HIV-1 Subtyping Tool, the distribution of HIV-1 genotypes in the study population was as follows: 32 cases (78%) of subtype B, two (4.9%) subtype C, two (4.9%) subtype G, four (9.8%) CRF02_AG, and one case (2.4%) of CRF01_AE.

To investigate the geographic origin of the Mongolian strains, the 41 *pol* sequences were compared against all HIV-1 sequences in the NCBI database using a BLAST similarity search. A distance-based phylogenetic tree (NJ tree) was constructed with 67 *pol* reference sequences (Fig. 1A). As shown in the phylogenetic tree of the *pol* gene region, the majority (78%) of the sequences belonged to subtype B, in which two distinct clusters, named cluster 1 and cluster 2, were identified. Twenty-one (65.6%) of the total 32 subtype B sequences, which included 16 MSM, two HSM, and one HSF Mongolians, were grouped into "cluster 1." This cluster showed a remarkable monophyly with a long branch against the other sequences and high bootstrap value (<98%). The mean nucleotide diversity within the cluster was low (<0.01), indicating that members of this cluster were closely related. Russian B strains (07RUS-K0511NOV07 and 07RUS-K0611NOV07) were included in cluster 1, suggesting a Russian carrier was responsible for the Mongolian HIV-1 epidemic. Cluster 2 consisted of sequences from eight (25%) MSM Mongolian patients and four reference strains from Korean subtype B origin. Cluster 2 was more divergent than cluster 1, and had a relatively low bootstrap value (<90%). We also identified three small groups, group 2a, 2b, and 2c, in cluster 2. They had high clade credibility (bootstrap value >98%) and low genetic divergences (<0.01).

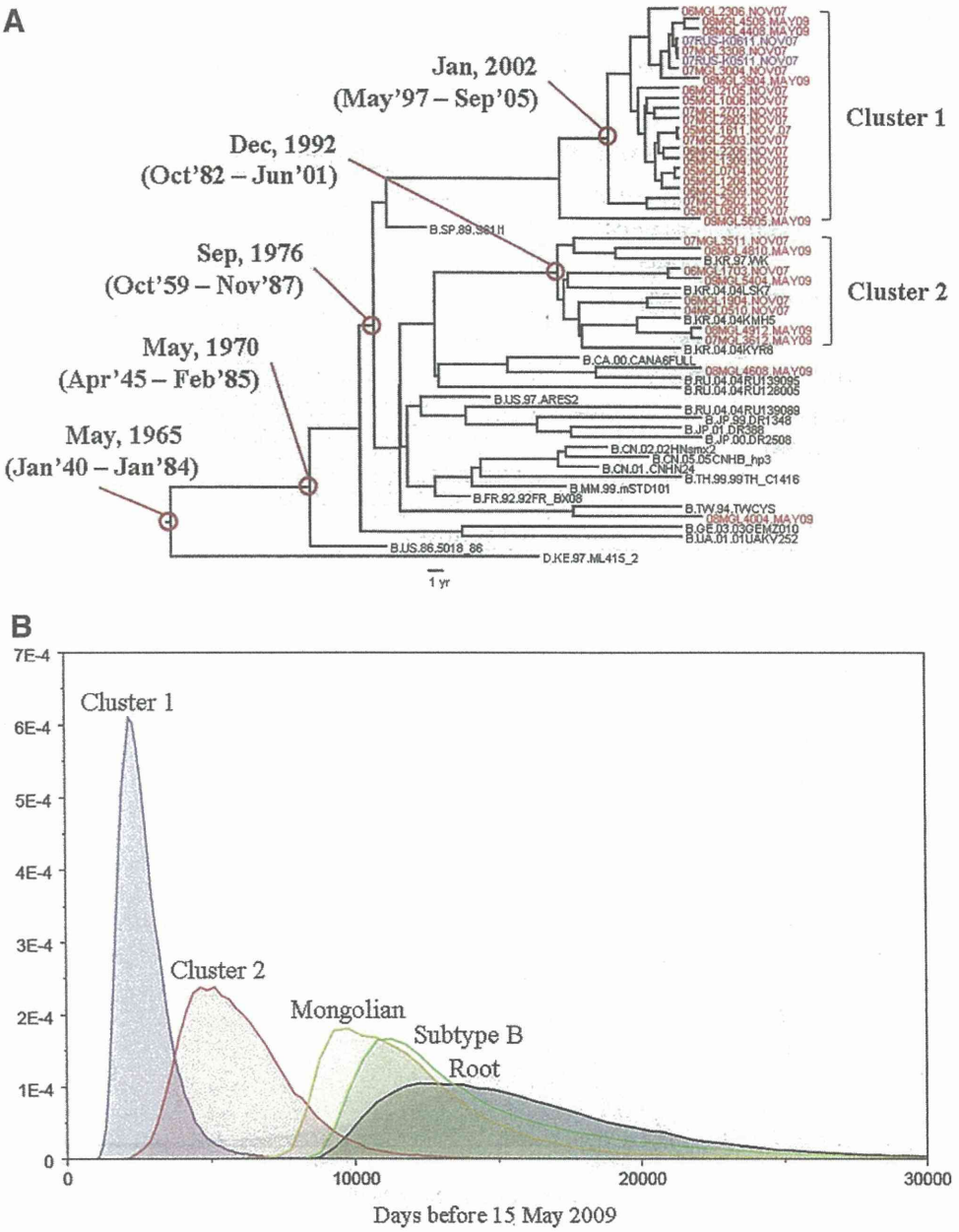

FIG. 3. Bayesian coalescence analysis of *pol* gene HIV-1 subtype B. **(A)** Maximum clade credibility tree of the *pol* gene by Bayesian Markov chain Monte Carlo (MCMC) analysis. The rooted tree illustrates the chronological phylogenetic relationship of 30 Mongolians and 22 reference HIV-1 subtype B *pol* (PR to RT; 1065 nt) sequences. The branch length of phylogeny is in units of time, and a yearly scale is shown under the tree. Red-purple sequence names represent the sequences in Mongolian and Russian patients, respectively. The clusters detected in the neighbor-joining (NJ) trees are annotated by brackets on the right of the tree. Month and year labels with red lines and circles indicate times of the most recent common ancestors (tMRCAs) of corresponding monophyletic groups, and the labels in parentheses indicate the 95% highest posterior density (HPD) interval of the tMRCA. **(B)** Marginal densities of tMRCAs on the Bayesian MCMC analysis. Blue, red, orange, green, and black represent the distribution of tMRCA estimates of cluster 1, 2, whole Mongolian subtype B, subtype B, and root height, respectively.

Two sequences isolated from two Mongolian heterosexual men belonged to subtype G. They were close relatives and seemed to have diverged from the reference sequences of subtype G of Central African (Nigeria) origin. All other remaining Mongolian sequences were from female patients. Two sequences (one was FSW) were close to the reference sequences subtype C of Asian (India) and Northeast African (Ethiopia and Burundi) origins, respectively. The sequences of four sex workers represented CRF02_AG. These sequences were close to reference strains isolated from Uzbekistan, Cameroon, and Ghana. The remaining isolated sequence was CRF01_AE, which was close to reference strains from Vietnam.

Twenty-eight out of the 32 subtype B samples based on the *pol* gene sequences were successfully amplified and the *env* (C2V3) gene region was sequenced and a phylogenetic tree was constructed (Fig. 1B). All samples were also classified as subtype B, indicating that they were not intersubtype recombinant forms if judged from the *pol* and *env* genes. Since the *env* gene region of HIV-1 has high sequence diversity, it is suitable for gene evolution analysis. Nevertheless, the intragroup nucleotide diversity of all 21 sequences on the *env* gene region in cluster 1 was very low, reflecting the rapid expansion of transmission of this lineage of HIV-1 in Mongolia. In contrast, seven other sequences on the *env* gene region belonging to cluster 2 were considerably divergent, suggesting a multiple origin of cluster 2.

Newly diagnosed cases of HIV-1 infection in Mongolia markedly increased in 2005 (Fig. 2, upper panel). Since that year, 7–13 new cases of HIV-1 infection had been diagnosed annually. Although the dominant subtype in Mongolia is currently subtype B, the first subtype-confirmed case in our analysis was CRF02_AG and was detected in 1997 (Fig. 2, lower panel). In 2004, one virus was classified into subtype B.

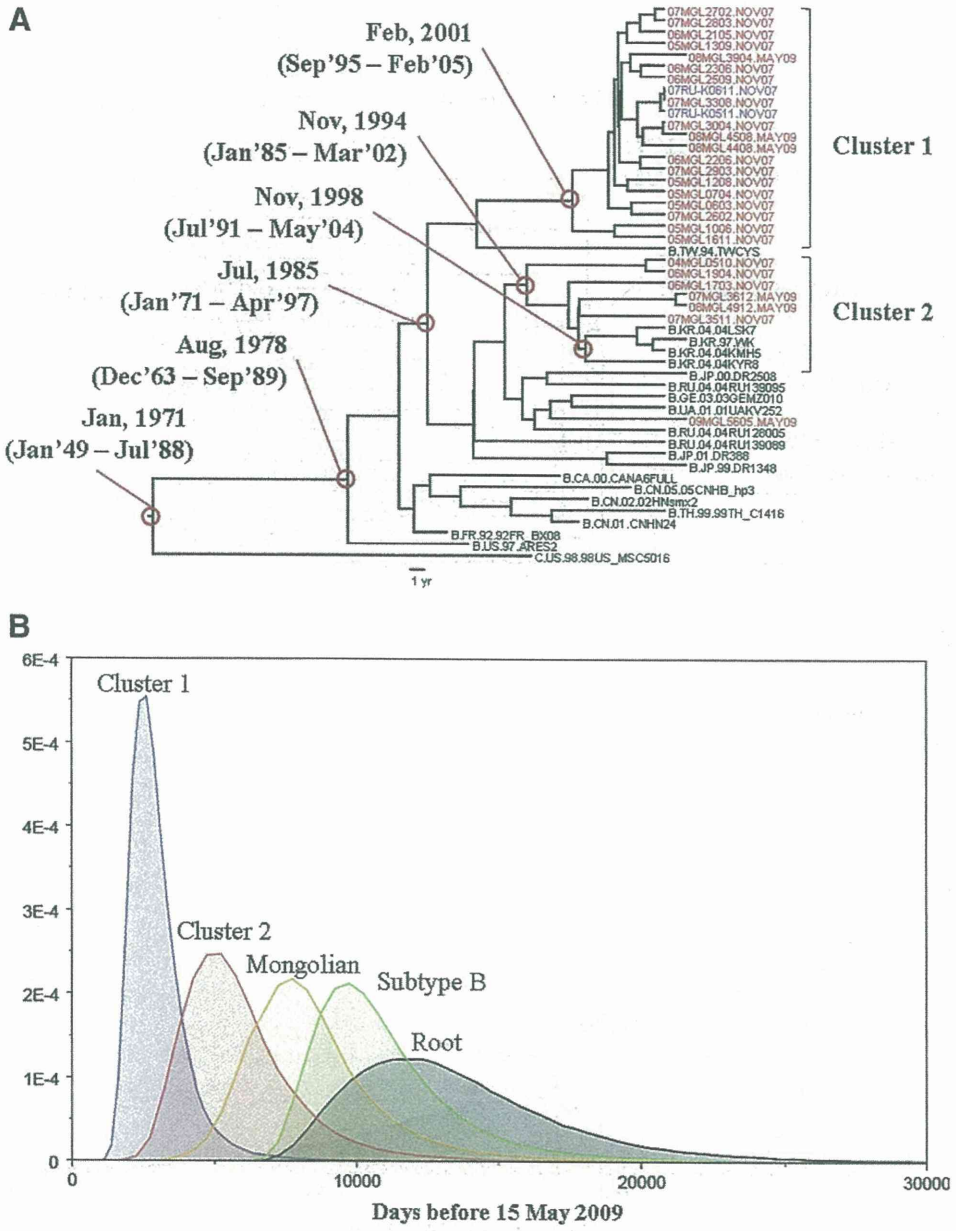

FIG. 4. Bayesian coalescence analysis of the *env* gene of subtype B. **(A)** Maximum clade credibility tree of the *env* gene by Bayesian MCMC analysis. The rooted tree illustrates the chronological phylogenetic relationship of 26 Mongolians and 23 reference HIV-1 subtype B *env* (C2V3; 447 nt) sequences. The branch length of the phylogeny is in units of time, and a yearly scale is shown under the tree. Red-purple sequence names represent the sequences of Mongolian and Russian patients, respectively. The clusters detected in the NJ trees are annotated by brackets on the right of the tree. Month and year labels with red lines and circles indicate tMRCAs of the corresponding monophyletic groups, and the labels in parentheses indicate 95% HPD confidence interval of the tMRCA. **(B)** Marginal densities of tMRCAs on the Bayesian MCMC analysis. Blue, red, orange, green, and black represent the distribution of tMRCA estimates of cluster 1, 2, whole Mongolian subtype B, subtype B, and root height, respectively.

This virus belonged to cluster 2, and was assumed to be of Korean origin. In 2005, viruses from six patients were classified as subtype B while one was subtype C and CRF02_AG, respectively. All subtype B viruses belonged to cluster 1 in our phylogenetic analysis. In 2006, viruses from six patients were also classified as subtype B, and two of them belonged to cluster 2. One of these cluster 2 viruses was also assumed to be of Korean origin (i.e., group 2c). From 2006, cluster 1 viruses had been twice as dominant as cluster 2 viruses. Other subtypes and CRFs were rarely collected in Mongolia.

To assess the result of the distance-based analysis, and to estimate tMRCAs of the Mongolian clusters, we performed a Bayesian coalescent-based phylogenetic inference. Appling the Bayesian relaxed molecular clock method to the phylogeny, the estimated mean evolutionary rates per year per site were 1.90×10^{-3} and 6.66×10^{-3} for *pol* and *env*, respectively (Supplementary Table S1; Supplementary Data are available online at www.liebertonline.com/aid). The estimated mean coefficients of variation were 0.72 and 0.48 for *pol* and *env*, indicating substantial heterogeneity in the evolutionary rate among viral lineage (Supplementary Table S1). The topology of the maximum clade credibility trees of both regions by the Bayesian MCMC analysis was similar to the NJ trees (Figs. 3 and 4), although some differences were observed between trees on the *pol* and *env* regions. One of these differences was found in Korean subtype B sequences in cluster 2. Thus, the Korean sequences formed a monophyletic group in the *pol* tree, but not in the *env* tree. Another notable difference was 09MGL5605.MSM.MAY09, which was close to cluster 1 in the *pol* tree but was related to cluster 2 in the *env* tree. The remaining differences were caused by differences in the samples used for analysis; while we were able to sequence 26 samples for the *env* region, 30 sequences were available for the *pol* region. The Bayesian chronological phylogenies showed that cluster 2 had older ancestors than cluster 1. Based on the estimates of the evolutionary rate, the mean tMRCA of cluster 1

was dated January 2002 on the *pol* region (Fig. 3A) and February 2001 on the *env* region (Fig. 4A). The marginal density of the posterior probabilities of tMRCA in both regions indicated that tMRCA of cluster 1 viruses ranged from 1995 to 2005 (Figs. 3B and 4B). On the other hand, the mean tMRCA of cluster 2 was dated December 1992 on the *pol* region (Fig. 3A) and November 1994 on the *env* region (Fig. 4A). The marginal density of tMRCA of cluster 2 was blunter than that of cluster 1, showing less reliability of tMRCA estimates of cluster 2. The root height of all Mongolian and U.S.-related subtype B reference sequences dated from the late 1960s to early 1970s.

Discussion

It is important to monitor circulating subtypes and the emerging genetic diversity of HIV-1 not only because it has implications for global surveillance but also because it should facilitate risk analysis of HIV-1 transmission and help effective strategies for HIV-1 prevention.[15–19]

The present study is the first report that provides definitive evidence of HIV-1 infection occurring in a low prevalence country, Mongolia. Our results showed that HIV-1 subtype B is responsible for nearly 78% of the analyzed samples, and possibly by sexual network within the predominant MSM (84.8%) risk group. The phylogenetic analyses of HIV-1 *pol* subtype B sequences from Mongolian and non-Mongolian origins showed that sequences of cluster 1 and cluster 2 formed monophyletic groups compared with other viruses of the same and different subtypes from around the world, indicating that HIV-1 subtype B entered Mongolia through two distinct origins.

The most intriguing feature of this epidemic is the very low genetic diversity of cluster 1. Molecular analysis strongly indicated that HIV-1 spread rapidly during a relatively short period with the same ancestor virus. Patients of cluster 1 were diagnosed between 2005 and 2008. However, the result of the Bayesian MCMC analyses suggests that the main outbreak occurred around the early 2000s. The short-term expansion also strongly suggests a high-risk sexual behavior in this population.[20] Although most patients were MSM, the group also included bisexual and female patients. They could potentially serve as a bridge between MSM and a lower-risk population, such as heterosexually active adults. Based on the extremely high prevalence of syphilis in FSW as determined in our nationwide surveillance of HIV/STI in 2007,[2] Mongolia is at high risk of an expansion of HIV-1 infection. In Russia, subtype B is not a major subtype in the total HIV epidemic but is predominant among MSM.[21] However, it is possible that the Russian subtype B strain may become the major strain in the Mongolian population in the future. Based on this, comprehensive preventive measures are urgently needed for this group and our team has already started taking action.

The median evolution rates estimated for Mongolian subtype B in the *pol* (1.9×10^{-3} substitution site per year) and *env* region (6.66×10^{-3} substitution site per year) were comparable with the rates reported previously for these genomic regions for subtype B in other countries (*pol* 2.5×10^{-3} substitution site per year,[22] *env* $5–7\times10^{-3}$ substitution site per year[23,24]). Considering these evolutionary rates, the older origin was probably from Korean HIV-1 subtype B, and first emerged in Mongolia around the early 1990s, almost a decade before the first detection of HIV-1 subtype B in Mongolia. However, this group also has the potential to be a major cluster in the future. This conclusion is based on the demographic data that documented that most of the patients in this group lived in South Korea as migrant workers. At present, more than 10,000 Mongolian migrant workers live and work in South Korea. They are usually young, sexually active, and living alone. Their working and living conditions are unstable and looking for friends and sex partners is not easy in a new environment. Given these circumstances, these workers are a vulnerable population for HIV-1 infection. These data clearly demonstrate that education on HIV-1 infection among the migrant workers is not enough and comprehensive actions for the prevention of HIV-1 infection are needed before these workers go abroad.

In conclusion, our study identified a hot spot of HIV-1 transmission expanding currently and the potential seed of the epidemic in Mongolia. Comprehensive preventive measures are crucial to keep the rate of HIV-1 infection low in Mongolia. Our study provided clues for effective strategic actions for HIV-1 prevention.

Acknowledgments

This study was supported by grants from the National Center for Global Health and Medicine (H20-04-R) from the Ministry of Health, Labour, and Welfare of Japan and from the Global Center of Excellence Program (Global Education and Research Center Aiming at the Control of AIDS) from the Ministry of Education, Science, Sports, and Culture of Japan. The authors would like to thank all the doctors and assistant nurses of the AIDS/STI Department NCCD, Mongolia, for their roles in enrolling study participants and collecting blood samples. We are also grateful to all participants who contributed to the study.

Author Disclosure Statement

No competing financial interests exist.

References

1. Ministry of Health Mongolia, Global Fund supported project on AIDS and TB: Second generation HIV/STI surveillance report–2007. Mongolia, 2007.
2. Davaalkham J, Unenchimeg P, Baigalmaa Ch, *et al.*: High-risk status of HIV-1 infection in the very low epidemic country, Mongolia, 2007. Int J STD AIDS 2009;20:391–394.
3. Bello G, Passaes CP, Guimarães ML, *et al.*: Origin and evolutionary history of HIV-1 subtype C in Brazil. AIDS 2008;22:1993–2000.
4. Gilbert MT, Rambaut A, Wlasiuk G, *et al.*: The emergence of HIV/AIDS in the Americas and beyond. Proc Natl Acad Sci USA 2007;104:18566–18570.
5. Worobey M, Gemmel M, Teuwen DE, *et al.*: Direct evidence of extensive diversity of HIV-1 in Kinshasa by 1960. Nature 2008;455:661–664.
6. Salemi M, de Oliveira T, Ciccozzi M, *et al.*: High-resolution molecular epidemiology and evolutionary history of HIV-1 subtypes in Albania. PLoS One 2008;3:e1390.
7. de Oliveira T, Deforche K, Cassol S, *et al.*: An automated genotyping system for analysis of HIV-1 and other microbial sequences. Bioinformatics 2005;21:3797–3800.
8. Tamura K, Dudley J, Nei M, and Kumar S: MEGA4: Molecular Evolutionary Genetics Analysis (MEGA) software version 4.0. Mol Biol Evol 2007;24:1596–1599.

9. Swofford DL: PAUP*. Phylogenetic Analysis Using Parsimony (*and Other Methods). Version 4. Sinauer Associates, Sunderland, Massachusetts, 2003.
10. Nylander JAA: MrModeltest v2. Program distributed by the author. Evolutionary Biology Centre, Uppsala University, 2004.
11. Rodríguez F, Oliver JL, Marín A, *et al.*: The general stochastic model of nucleotide substitution. J Theor Biol 1990;142:485–501.
12. Drummond AJ and Rambaut A: BEAST: Bayesian evolutionary analysis by sampling trees. BMC Evol Biol 2007; 7:214.
13. Drummond AJ, Ho SY, Phillips MJ, *et al.*: Relaxed phylogenetics and dating with confidence. PLoS Biol 2006;4:e88.
14. Pybus OG, Drummond AJ, Nakano T, *et al.*: The epidemiology and iatrogenic transmission of hepatitis C virus in Egypt: A Bayesian coalescent approach. Mol Biol Evol 2003;20:381–387.
15. Bennett D: HIV [corrected] genetic diversity surveillance in the United States. J Infect Dis 2005;192:4–9.
16. de Oliveira T, Pybus OG, Rambaut A, *et al.*: Molecular epidemiology: HIV-1 and HCV sequences from Libyan outbreak. Nature 2006;444:836–837.
17. Hu DJ, Dondero TJ, Rayfield MA, *et al.*: The emerging genetic diversity of HIV. The importance of global surveillance for diagnostics, research, and prevention. JAMA 1996;275: 210–216.
18. Hué S, Clewley JP, Cane PA, *et al.*: HIV-1 pol gene variation is sufficient for reconstruction of transmissions in the era of antiretroviral therapy. AIDS 2004;18:719–728.
19. Peeters M, Toure-Kane C, and Nkengasong JN: Genetic diversity of HIV in Africa: Impact on diagnosis, treatment, vaccine development and trials. AIDS 2003;17:2547–2560.
20. Maljkovic Berry I, Ribeiro R, Kothari M, *et al.*: Unequal evolutionary rates in the human immunodeficiency virus type 1 (HIV-1) pandemic: The evolutionary rate of HIV-1 slows down when the epidemic rate increases. J Virol 2007;81:10625–10635.
21. Bobkov AF, Kazennova EV, Selimova LM, *et al.*: Temporal trends in the HIV-1 epidemic in Russia: Predominance of subtype A. J Med Virol 2004;74:191–196.
22. Hué S, Pillay D, Clewley JP, *et al.*: Genetic analysis reveals the complex structure of HIV-1 transmission within defined risk groups. Proc Natl Acad Sci USA 2005;102:4425–4429.
23. Leitner T and Albert J: The molecular clock of HIV-1 unveiled through analysis of a known transmission history. Proc Natl Acad Sci USA 1999;96:10752–10757.
24. Robbins KE, Lemey P, Pybus OG, *et al.*: U.S. human immunodeficiency virus type 1 epidemic: Date of origin, population history, and characterization of early strains. J Virol 2003;77:6359–6366.

Address correspondence to:
Davaalkham Jagdagsuren
AIDS Clinical Center
National Center for Global Health and Medicine
1-21-1, Toyama, Shinjuku-ku
Tokyo 162-8655
Japan

E-mail: jdavaalkham@yahoo.com

European Journal of Immunology

Selection of escape mutant by HLA-C-restricted HIV-1 Pol-specific cytotoxic T lymphocytes carrying strong ability to suppress HIV-1 replication

Kazutaka Honda[1], Nan Zheng[1], Hayato Murakoshi[1], Masao Hashimoto[1], Keiko Sakai[1], Mohamed Ali Borghan[1,2], Takayuki Chikata[1], Madoka Koyanagi[1], Yoshiko Tamura[1], Hiroyuki Gatanaga[1,3], Shinichi Oka[1,3] and Masafumi Takiguchi[1]

[1] Center for AIDS Research, Kumamoto University, Honjo, Kumamoto, Japan
[2] Department of Biological Sciences, College of Arts and Sciences, University of Nizwa, Oman
[3] AIDS Clinical Center, National Center for Global Health and Medicine, Toyama, Shinjuku-ku, Tokyo, Japan

HIV-1 mutants escaping from HLA-A- or HLA-B-restricted CTL have been well studied, but those from HLA-C-restricted CTL have not. Therefore we investigated the ability of HLA-C-restricted CTL to select HIV-1 escape mutants. In the present study, we identified two novel HLA-Cw*1202-restricted Pol-specific CTL epitopes (Pol328-9 and Pol463-10). CTL specific for these epitopes were detected in 25–40% of chronically HIV-1-infected HLA-Cw*1202$^+$ individuals and had strong abilities to kill HIV-1-infected cells and to suppress HIV-1 replication *in vitro*, suggesting that these CTL may have the ability to effectively control HIV-1 in some HLA-Cw*1202$^+$ individuals. Sequence analysis of these epitopes showed that a V-to-A substitution at the 9th position (V9A) of Pol 463-10 was significantly associated with the HLA-Cw*1202 allele and that the V9A mutant was slowly selected in the HLA-Cw*1202$^+$ individuals. Pol 463-10-specific CTL failed both to kill the V9A virus-infected cells and to suppress replication of the V9A mutant. These results indicate that the V9A mutation was selected as an escape mutant by the Pol463-10-specific CTL. The present study strongly suggests that some HLA-C-restricted CTL have a strong ability to suppress HIV-1 replication so that they can select HIV escape mutants as in the case of HLA-A-restricted or HLA-B-restricted CTL.

Key words: CTL · Escape mutation · Fitness · HLA-C · HIV infection

Supporting Information available online

Introduction

CTL are involved in the control of HIV-1 replication during acute and chronic phases of HIV-1 infections [1–8]. However, CTL cannot completely eradicate HIV-1 because HIV-1 escapes from the cell-mediated immune system of the host by various mechanisms [9–17]. One such mechanism is the appearance of a single amino acid mutation within CTL epitopes, which is crucial for preventing their binding to HLA class I molecules or for the interaction between the TCR of the HIV-1-specific CTL and the peptide-HLA class I complex. The escape mechanisms result in the loss of CTL activities against HIV-1-infected target cells and

Correspondence: Prof. Masafumi Takiguchi
e-mail: masafumi@kumamoto-u.ac.jp

contribute to the selection of viruses capable of escaping from HIV-1-specific CTL [4, 9–11, 18, 19]. Many studies demonstrated that the immune pressure mediated by HIV-1-specific CTL selects escape variants during both acute and chronic HIV-1 infections and that the selection of escape mutants could result in the loss of immune control, leading to progression to AIDS [9, 20–25].

The majority of previous studies concerning HIV-1-specific CTL focused on HLA-A- or HLA-B-restricted ones. However, the role of HLA-C-restricted CTL in HIV infections has not been well documented. It is speculated that HLA-C-restricted CTL do not contribute to the control of HIV-1 replication, because the expression level of HLA-C molecules is approximately 10% of that of HLA-A or -B molecules [26, 27]. In contrast, HIV-1 Nef-mediated HLA class I down-regulation affects HLA-A- or HLA-B-restricted CTL recognition but not the HLA-C-restricted one [28], suggesting a role for the HLA-C allele in HIV-1 infections. In addition, a whole-genome association study indicated that a variant located 35 kb upstream of the HLA-C gene (rs9264942) is associated not only with HLA-C mRNA expression but also with HIV viral load (VL) and AIDS progression [29, 30]. These studies suggest that the HLA-C-restricted immune responses play an important role in the control of HIV-1.

There are very few studies on HIV-1-specific HLA-C-restricted T cells. A previous study using HIV-1-specific HLA-C-restricted CTL clones demonstrated that HLA-HLA-C*03, 07, 15-restricted HIV-1-specific CTL clones effectively suppress HIV-1 replication *in vitro* [28]. A recent study revealed that HLA-C*04-restricted CTL have functional and phenotypic characteristics similar to those of HLA-A or B-restricted CTL [31]. Previous population analyses showed the association of some HLA-C alleles with the substitutions of HIV [32, 33]. Although these studies suggest the possibility that HLA-C-restricted CTL can select HIV-1 escape mutants, they did not directly show that HLA-C-restricted CTL actually do so.

In the present study, we investigated whether HLA-C-restricted CTL could select escape mutants. We focused on HLA-Cw*1202-restricted CTL because this allele, which forms a haplotype with HLA-A*2402 and HLA-B*5201, is frequently detected in Japan. To clarify the role of HLA-Cw*1202-restricted CTL in the selection of escape mutants, we first identified HLA-Cw*1202-restricted epitopes and then measured the ability of the HLA-Cw*1202-restricted CTL to suppress HIV-1 replication. Furthermore, we analysed mutations of HIV that had escaped from the CTL.

Results

Identification of 2 HLA-Cw*1202-restricted HIV-1 Pol-specific CTL epitopes

To identify HLA-Cw*1202-restricted CTL epitopes, we stimulated PBMC from chronically HIV-1-infected donor KI-069 (HLA-A*2402/-, B*5201/4006, Cw*1202/0304) with peptide cocktails including eight 17-mer overlapping peptides from Gag and Pol regions of HIV-1 and cultured the cells for 12–14 days. After stimulation with autologous B-lymphoblastoid cell lines (B-LCL) prepulsed with the corresponding peptide cocktail, each bulk culture was assessed by performing the intracellular cytokine assay. Bulk cultures from KI-069 responded specifically to 1 Gag cocktail, 3 Pol cocktails, and 3 Nef cocktails (data not shown). Further analysis using a single peptide demonstrated that 2 Gag (Gag 17–13 and Gag 17–14) and 3 Pol (Pol 17–40, Pol 17–48, and Pol 17–78) induced specific $CD8^+$ T cells responses (data not shown). HLA restriction of these T-cell responses was subsequently determined using a panel of B-LCL sharing 1 HLA class allele with KI-069. The results showed that $CD8^+$ T-cell responses against Gag 17-13, Pol 17–48, and Pol 17–78 peptides were restricted by a haplotype of HLA-A*2402, HLA-B*5201, and HLA-Cw*1202 (data not shown). Further analysis using C1R transfectant cells expressing each HLA molecule showed that only responses of $CD8^+$ T cells specific for the Pol 17–78 peptide were restricted by HLA-Cw*1202 (Fig. 1A top). Next, we generated a panel of 11-mer peptides covering the 17-mer amino acid sequences of the Pol 17–78 peptide and then tested IFN-γ production of each bulk culture in response to C1R-HLA-Cw*1202 cells prepulsed with these 11-mer peptides. Only the Pol 11–232 peptide induced the specific responses (Fig. 1A middle). To determine minimum length of the epitope, we generated four truncated peptides, Pol 11-232(IV9), Pol 11-232(C9), Pol 11-232(N10), and Pol 11-232(C10). Pol11-232-induced $CD8^+$ T cells recognised Pol 11-232(C10) but neither the IV9 nor the C9 (Fig. 1A bottom), indicating Pol 11-232(C10) to be the optimal epitope.

On the other hand, the ELISPOT assay using 11-mer overlapping Nef, Gag, and Pol peptides for KI-108 carrying HLA-A*2402/A*2402, B*5201/B*5201, and Cw*1202/Cw*1202 showed that 3 Pol peptide cocktails (Pol11-G17, Pol11-G27, and Pol11-G47) induced specific CD8 T-cell responses from this patient (data not shown). Subsequent analysis using single 11-mer peptides demonstrated that Pol11-164, Pol11-263, and Pol11-463 peptide-specific $CD8^+$ T cells were included among the PBMC cultured with Pol11-G17, Pol11-G27, and Pol11-G47, respectively (data not shown). In order to determine HLA class I restriction molecules of these peptide-specific T-cell responses, we employed C1R transfectants expressing each HLA molecule as stimulator cells and found that only Pol11-164-specific T-cell response was restricted by HLA-Cw*1202 (Fig. 1B top). To identify the optimal epitope recognised by $CD8^+$ T cells specific for Pol11-164, we synthesised a set of truncated peptides, Pol 11-164(RY10), Pol 11-164(RI9), Pol 11-164(KY9), Pol 11-164(QY8), and Pol11-164(KQ10) and tested which peptide the bulk cultured cells recognise. Pol 11-164(RY10), Pol 11-164(KY9), and Pol11-164(KQ10) peptides induced high IFN-γ responses of $CD8^+$ T cells in the culture (Fig. 1B middle). In addition, the analysis of peptide titration showed that the Pol11-164(KY9) peptide induced stronger IFN-γ responses of the $CD8^+$

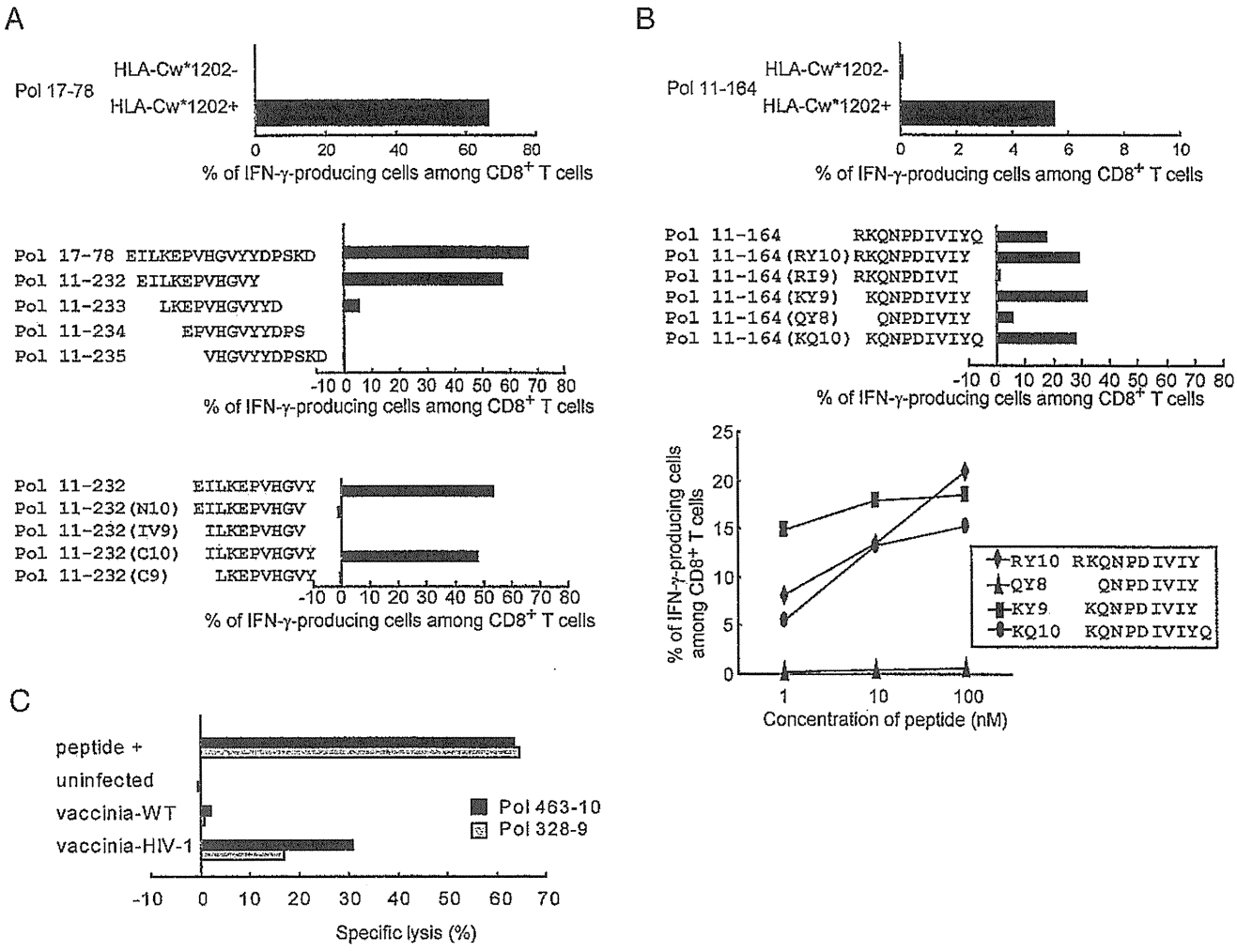

Figure 1. Identification of two HIV-1 Pol-specific epitopes using overlapping peptides. Candidates of HLA-Cw*1202-restricted HIV-1 CTL epitopes were identified using overlapping 17-mer or 11-mer HIV-1 peptides. PBMC from HLA-Cw*1202$^+$ HIV-1-seropositive individuals (KI-069 and KI-108) were stimulated with the 17-mer peptide cocktails and the 11-mer peptide cocktails, respectively, and then cultured for 12–14 days. (A) Top: A candidates of 17-mer Pol epitope peptide. The cultured PBMC cells form KI-069 were stimulated with the corresponding peptide-pulsed C1R cells expressing HLA-Cw*1202 (Cw*1202$^+$) or C1R cells (Cw*1202$^-$). Middle: Identification of 11-mer HIV-1 Pol peptides including HLA-Cw*1202-restricted epitope. The 17-mer cocktail peptide-specific bulk CD8$^+$ T cells were stimulated with C1R-Cw*1202 cells prepulsed with each of four overlapping 11-mer peptides. Bottom: Recognition of the 9-mer and 10-mer truncated peptides by the 11-mer-specific CD8$^+$ T cells. The 11-mer cocktail peptide-specific bulk CD8$^+$ T cells were stimulated with C1R-Cw*1202 prepulsed with each 8- to 10-mer truncated peptide. Peptide-specific CD8$^+$ T cells were detected using the intracellular IFN-γ staining assay. The percentages of IFN-γ-producing cells among CD8$^+$ T cells are shown at each figure. Each bar presents the data from one bulk T cells in a single experiment. (B) Top: A candidates of 11-mer Pol epitope peptides. The cultured PBMC cells from KI-108 were stimulated with the corresponding peptide-pulsed C1R cells expressing HLA-Cw*1202 (Cw*1202$^+$) or C1R cells (Cw*1202$^-$). Middle and Bottom: Pol11-164-specific bulk CTL were co-cultured with C1R-Cw*1202 prepulsed with each truncated peptide at concentrations of 100 nM (middle) or from 1 to 100 nM (bottom). The responsiveness of the bulk CD8$^+$ T cells toward each truncated peptide was measured by conducting the intracellular IFN-γ staining assay. The percentages of IFN-γ-producing cells among CD8$^+$ T cells are shown at each figure. Each bar or graph presents the data from one bulk T cells in a single experiment. (C) Presentation of two Pol epitopes by HLA-Cw*1202 on C1R-Cw*1202 cells infected with HIV-1 recombinant-HIV-1 vaccinia virus. The CTL activity of Pol 328-9-specific and Pol 463-10-specific bulk T cells against C1R-Cw*1202 cells prepulsed with a 1 μM concentration of the epitope peptide (peptide+) or infected with recombinant vaccinia virus expressing the corresponding HIV-1 Gag/Pol proteins (vaccinia-HIV-1) or WT vaccinia virus (vaccinia WT) was tested at an E:T ratio of 2:1. Each bar presents the data from one bulk T cells in a single experiment.

T cells than Pol the 11-164(RY10) or Pol 11-164(KQ10) one (Fig. 1B bottom). These results indicate that Pol 11-164(KY9) is the optimal epitope.

To clarify whether these two peptides were endogenously processed and presented by HLA-Cw*1202, we generated CTL clones specific for Pol 11-164(KY9) [9-mer peptide starting from position 328: Pol 328-9] or Pol 11-232(C10) [10-mer peptide starting from position 463: Pol 463-10], and then investigated whether these CTL clones could kill C1R-HLA-Cw*1202 cells infected with recombinant vaccinia virus expressing the HIV-1 Gag/Pol protein. These CTL clones effectively killed C1R-Cw*1202 infected with the recombinant vaccinia virus, but not those cells infected with WT vaccinia or uninfected cells (Fig. 1C), indicating that Pol 328-9 and Pol 463-10 are naturally processed CTL epitopes.

Frequency of HLA-Cw*1202-restricted HIV-1-specific CD8$^+$ T cells in chronically HIV-1-infected individuals

Next we investigated the frequency of the two Pol-specific HLA-Cw*1202-restricted CTL in chronically HIV-1-infected individuals carrying HLA-Cw*1202 in order to clarify whether they were immunodominant epitopes. We detected Pol 328-9-specific and Pol 463-10-specific T cells *ex vivo* among CD8$^+$ T cells from the HLA-Cw*1202$^+$ individuals by performing the ELISPOT assay (Fig. 2). Ten of 25 individuals tested showed positive responses for the Pol328-9 epitope. Since Pol 463-9 (ILKEPVHGV) is reported to be an HLA-A*02 epitope [34], we selected HLA-Cw*1202$^+$ individuals who did not have HLA-A*02 for Pol 463-10-specific T cells. Four of 15 individuals carrying HLA-Cw*1202 but not HLA-A*02 showed positive responses for Pol463-10. These indicate that the specific T cells were frequently elicited in chronically HIV-1-infected individuals carrying HLA-Cw*1202.

Strong abilities of HLA-Cw*1202-restricted CTL clones to suppress HIV-1 replication

To investigate the ability of HLA-C*1202-restricted HIV-1-specific CTL to suppress HIV-1 replication, we measured the ability of CTL clones specific for Pol 328-9 or Pol 463-10 to suppress HIV-1 replication in primary CD4$^+$ T cells infected with HIV-1 NL432. Three Pol 328-9-specific HLA-Cw*1202-restricted and three Pol 463-10-specific HLA-Cw*1202-restricted CTL clones completely suppressed HIV-1 replication at an E:T ratio of 1:1 (Fig. 3). Our previous studies showed that approximately 70% of HLA-A-restricted or HLA-B-restricted CTL clones weakly suppress HIV-1 replication (less than 50% suppression at E:T ratio of 1:1), whereas others such as HLA-B*5101-restricted Pol 283-specific and HLA-A*2402-restricted Nef 138-specific ones strongly suppress it (Supporting Information Table 1) [12, 35–37]. These results show that the two HLA-Cw*1202-restricted CTL had a strong ability to suppress HIV-1 replication *in vitro*.

Pol 463-10-9A is a mutant that escaped from Pol 463-10-specific CTL

To clarify whether Pol 328-9-specific or Pol 463-10-specific CTL select escape mutants at the population level, we analysed the sequences of these epitopes and their flanking regions in viruses from HLA-Cw*1202$^+$ and HLA-Cw*1202 HIV-1 infected-donors. Analysis of 16 HLA-Cw*1202$^+$ and 66 HLA-Cw*1202$^-$ individuals showed that several mutations were found in the Pol 328-9 epitope region (data not shown), but these mutations were not significantly associated with HLA- Cw*1202 ($p > 0.05$). We also analysed the sequence of Pol 463-10 from 133 HLA-Cw*1202$^+$ and 108 HLA-Cw*1202$^-$ HIV-1 infected-donors. Several mutations were found at positions 3 and 9 (Fig. 4A). The frequency of the 9A mutation was significantly higher in the HLA-Cw*1202$^+$ donors than in the HLA-Cw*1202$^-$ ones ($p = 0.001$, Fig. 4A), suggesting that the 9A was a mutant that escaped from the Pol 463-10-specific CTL. Since Pol 463-9 (ILKEPVHGV) is known to be an HLA-A*02 epitope [34], the 9A may be selected by Pol 463-9-specific HLA-A*02-restricted CTL. To clarify this possibility, we analysed the sequences at this position from 55 HLA-A*02$^+$ and 88 HLA-A*02$^-$ HIV-1-infected donors. Frequencies of HLA-A*02$^+$ and HLA-A*02$^-$ individuals having the 9A are 10.9 and 19.8%, respectively, indicating that HLA-A*02 is not significantly associated with the 9A mutation. Indeed, the 9A mutation has not been reported as escape mutant from Pol 463-9-specific HLA-A*02-restricted CTL. Further analysis of 26 HLA-Cw*1202$^+$ HLA-A*02$^-$ and 60 HLA-Cw*1202$^-$ HLA-A*02$^-$ HIV-1-infected-donors showed that the frequency of the 9A mutation was significantly higher in the HLA-Cw*1202$^+$ HLA-A*02$^-$ donors

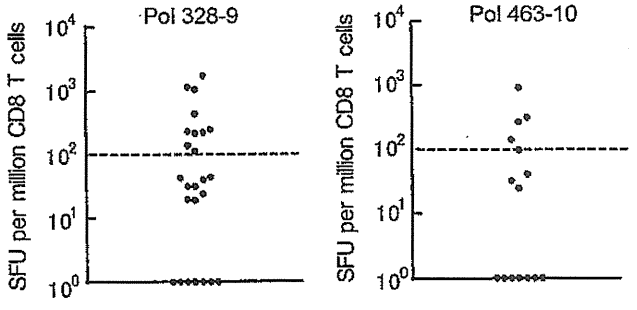

Figure 2. Frequency of HLA-Cw*1202-restricted Pol epitopes-specific CD8$^+$ T cells in chronically HIV-1-infected individuals. The frequencies of Pol 328-9-specific and Pol 463-10-specific CD8$^+$ T lymphocytes in chronically HIV-1-infected HLA-Cw*1202$^+$ individuals were measured using IFN-γ ELISPOT. Ten of 25 individuals tested showed positive responses for Pol328-9 epitope (mean SFU = 234), whereas four of 15 individuals who did not have HLA-A2 tested showed positive responses for Pol463-10 (mean SFU = 121). The subjects revealing a response of less than 100 SFU were evaluated as non-responders. SFU: spot-forming unit. Each dot represents one individual.

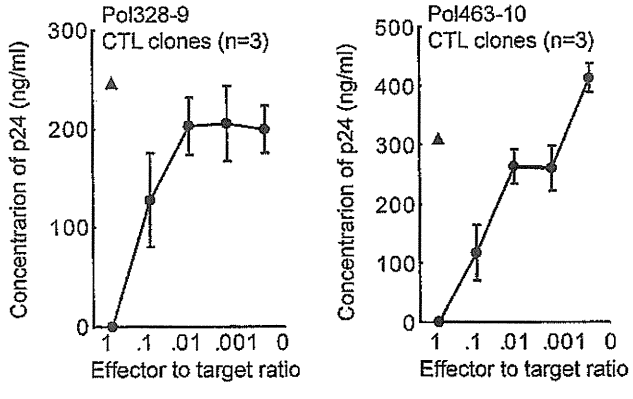

Figure 3. Strong abilities of two HIV-1 Pol-specific CTL to suppress HIV-1 replication. CD4$^+$ T cells from an HLA-Cw*1202$^+$ donor were infected with NL-432, and then co-cultured with the Pol-specific CTL clones ($n = 3$) at E:T ratios of 1:1, 0.1:1, 0.01:1, and 0.001:1 (circles). As a negative control, HLA-A*1101-restricted Pol675-specific CTL clone ($n = 1$) was used at an E:T ratio of 1:1 (triangle). HIV-1 p24 Ag in the supernatant were measured on day 7 after infection by an enzyme immunoassay. The data shown are the means and SD of assays for three HIV-1-specific CTL clones. They were from one out of two independent experiments.

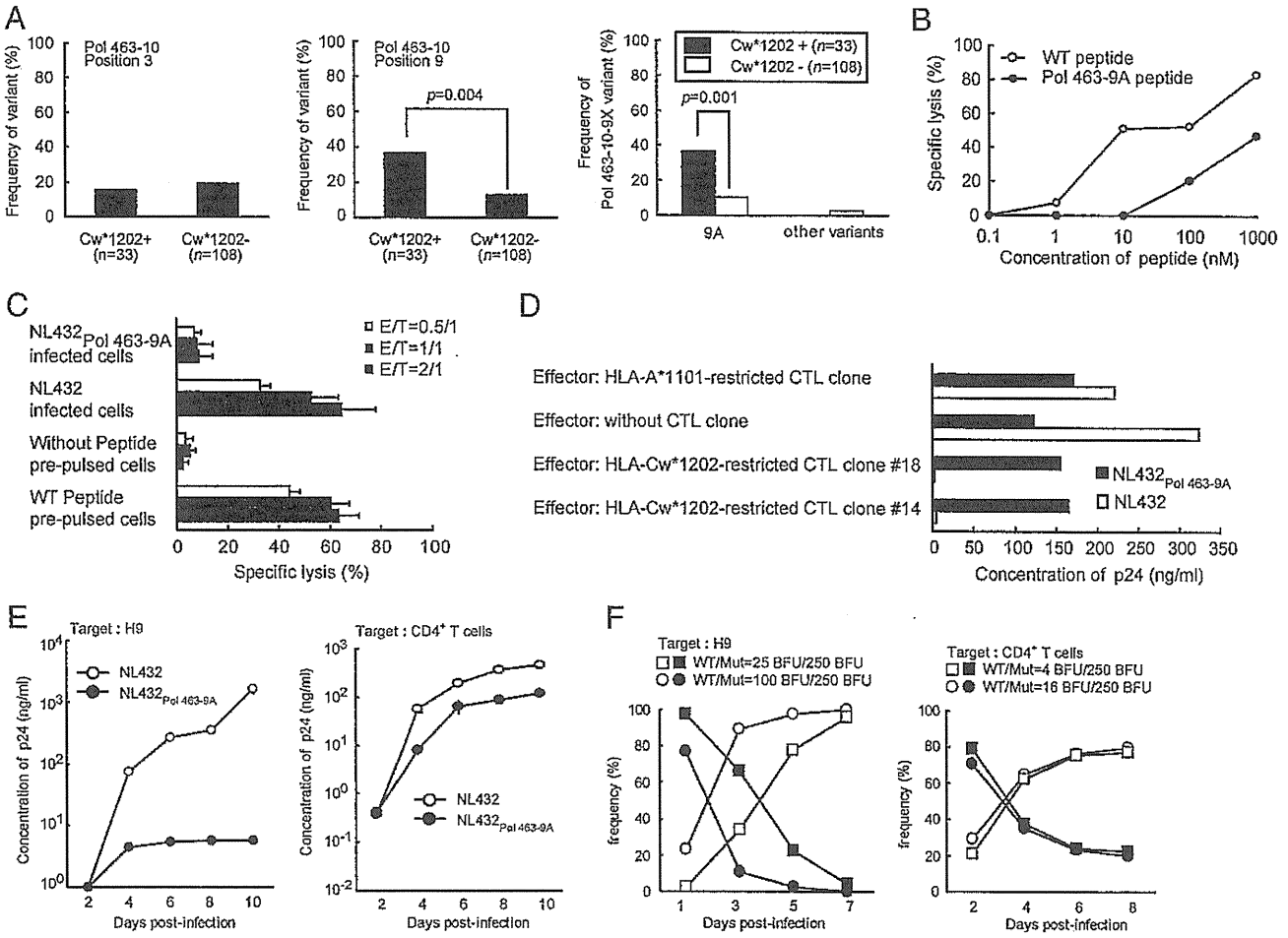

Figure 4. Characterization of escape Pol 463-9A escape mutation. (A) Frequency of mutations in Pol 463-10 epitope among chronically HIV-1-infected HLA-Cw*1202$^+$ and HLA-Cw*1202$^-$ HIV-1-infected individuals. The sequence of Pol 463-10 epitope was analysed in a single sample from both HLA-Cw*1202-positive or HLA-Cw*1202-negative individuals chronically infected with HIV-1. Thirty-three HLA-Cw*1202-positive or 108 HLA-Cw*1202-negative individuals were analysed. The consensus sequence of the Pol 463-10 epitope in clade B is ILKEPVHGVY. The frequency of mutations at positions 3 and 9 of the epitope are shown for both HLA-Cw*1202-positive and HLA-Cw*1202-negative donors. Frequency of Ala mutation at position 9 was significantly higher in HLA-Cw*1202-positive donors than in HLA-Cw*1202-negative donors. The p values were determined by Fisher's exact test. (B) Cytotoxic activities of Pol463-10-specific CTL clone toward C1R-HLA-Cw*1202 cells pulsed with Pol 463-10 or Pol 463-10-9A peptide. C1R-Cw*1202 cells were prepulsed with various concentrations of Pol 463-10 or Pol 463-10-9A peptide. Cytotoxic activity of a Pol463-10-specific CTL clone was measured at an E:T ratio of 2:1. The results were from a single T cell clone in one of two independent experiments. (C) Cytotoxic activity of Pol 463-10-specific CTL clones against 721.221-CD4-HLA-Cw*1202 cells infected with the 9A mutant virus; 721.221-CD4- HLA-Cw*1202 cells were infected with NL-432 or NL-432 $_{\text{Pol 463-10-9A}}$ mutant virus. NL-432-infected or NL-432 $_{\text{Pol 463-10-9A}}$-infected 721.221-CD4-HLA-Cw*1202 were used as target cells at an E:T ratio of 2:1, 1:1, or 0.5:1. The data shown are the means and SD of assays for three HIV-1-specific CTL clones. They were from one of two independent experiments. (D) Ability of HIV-1-specific CTL clones to suppress HIV-1 replication in the 9A mutant virus-infected CD4$^+$ T cells. CD4$^+$ T cells from an HLA-Cw*1202$^+$ HLA-A*1101$^-$ healthy donor were infected with NL-432 or NL-432 $_{\text{Pol 463-10-9A}}$, and then co-cultured with the Pol 463-10-specific CTL clone (clone #14 or clone #18) or HLA-A*1101-restricted CTL clone at an E:T ratio of 2:1 or without the CTL clone. HIV-1 p24 Ag in the supernatant were measured on day 7 after infection by performing an enzyme immunoassay. The results were from one T-cell clone in one of two independent experiments. (E) Fitness of the 9A mutant virus. Production of p24 Ag in culture supernatant was determined by an enzyme immunoassay. Profiles of replication kinetics (p24 production) of NL-432 (closed circles), NL-432 $_{\text{Pol 463-10-9A}}$ (open circles) were determined with H9 cells and CD4$^+$ T cells. The data shown are the means and SD of triplicates in one of two independent experiments. (F) A competitive HIV-1 replication assay using the 9A mutant and WT virus. To compare the replication kinetics of NL-432 (open symbols) and NL-432 $_{\text{Pol 463-10-9A}}$ (closed symbols), H9 cells (left), and CD4$^+$ T cells (right) were infected with both viruses at different viral titers. The frequency of each virus at day 1, 3, 5, and 7 (H9 cells) or at day 2, 4, 6, and 8 (CD4$^+$ T cells) was determined from the relative peak height on sequencing electrograms. The data were from one sample in a single experiment.

than in the HLA-Cw*1202$^-$HLA-A*02$^-$ ones (34.6 *versus* 14.4%, $p = 0.037$). These results together suggest that HLA-Cw*1202-restricted Pol 463-10-specific CTL selected the 9A mutant.

To clarify whether the 9A was indeed an escape mutant of Pol 463-10-specific CTL, we investigated the ability of Pol 463-10-specific CTL to recognise the Pol 463-10-9A mutant epitope. We first tested the activity of Pol 463-10-specific CTL clones to kill target cells prepulsed with the Pol 463-10-9A mutant peptide. Three Pol 463-10-specific CTL clones effectively killed target cells prepulsed with the Pol 463-10 WT peptide but showed reduced ability to kill those prepulsed with the Pol 463-10-9A mutant peptide (Fig. 4B), suggesting that the 9A mutant had escaped

Table 1. Longitudinal analysis of Pol 463-10 epitope sequence in HIV-1-infected individuals

ID	HLA-Cw*1202	Sample date Month/day/year	Sequence ILKEPVHGVY
KI-037	Positive	01/29/2002	----------
		06/17/2004	--------A-
KI-163	Positive	08/30/2002	----------
		06/28/2004	----------
		08/29/2005	--------A-
		02/27/2006	--------A-
KI-428	Positive	03/12/2003	----------
		06/28/2006	----------
		09/27/2006	----------
		07/12/2007	--------A-
KI-452	Positive	12/30/1999	----------
		01/30/2007	--------A-
KI-097	Negative	04/25/2003	--------A-
		02/18/2005	--R-------
KI-091	Negative	09/10/2001	--------A-
		07/09/2003	--R-------
KI-161	Negative	07/25/2002	--E-----A-
		05/07/2004	----------
		09/29/2004	----------

from Pol 463-10-specific CTL. Therefore we generated the 9A mutant virus from NL432 (NL-432-$_{\text{Pol 463-10-9A}}$) to further analyse the ability of Pol 463-10-specific CTL to kill target cells infected with the 9A mutant virus. The Pol 463-10-specific CTL clones effectively killed the target cells infected with NL-432 whereas they failed to kill those infected with NL-432-$_{\text{Pol 463-10-9A}}$ (Fig. 4C). In addition, by performing a replication suppression assay we analysed whether these CTL could suppress the replication of mutant virus and WT virus *in vitro*. Pol 463-10-specific CTL clones (clone #14 and #18) effectively suppressed the replication of the WT virus, whereas they failed to suppress that of the 9A mutant virus (Fig. 4D). These results indicate that the 9A is indeed escape mutant of Pol 463-10-specific CTL.

We performed longitudinal analysis of the Pol 463-10 epitope in 14 HLA-Cw*1202$^+$ individuals. Four HLA-Cw*1202$^+$ individuals showed the WT sequence of Pol 463-10 in the early phase and the Pol 463-10-9A mutant appeared more than 3 years later (Table 1), supporting that the 9A is escape mutant from Pol 463-10-specific CTL. KI-037 is a haemophiliac patient who had been infected with HIV-1 before 1985, indicating that the 9A mutant appeared more than 17 years after HIV-1 infection. Thus, this mutant may be slowly selected in HLA-Cw*1202$^+$ individuals.

Reversion of the 9A mutant

To examine the effect of the 9A mutation on viral fitness, we compared the replication ability of NL432 (WT) and the 9A mutant using the p24 production assay. The results using H9 cells and primary CD4$^+$ T cells as target cells showed that fitness cost of the 9A was much higher than that of WT (Fig. 4E). In addition, we performed a competitive HIV-1 replication assay for further comparison of replication kinetics in H9 cells and primary CD4$^+$ T cells. During 7 days culture, we observed that the 9A had higher fitness cost than WT in both cells (Fig. 4F). These results suggest that this mutant is able to revert to WT in HLA-Cw*1202$^-$ HIV-1-infected individuals. To clarify the reversion, we performed a longitudinal analysis of this epitope sequence on five HLA-Cw*1202$^-$ individuals who could be followed from early stage of the infection and had the 9A mutation at the early stage. Three of these five HLA-Cw*1202$^-$ individuals showed the reversion within approximately 2 years after the 9A had been found (Table 1). These results support the finding that the 9A mutant did not remarkably accumulate in the HLA-Cw*1202$^-$ individuals.

Discussion

HLA-C molecules are believed to play a less important role in the presentation of various Ag than HLA-A and -B ones, because the former molecules are expressed on the cell surface at a level that is approximately 10% of that of the latter molecules [26, 27]. On the other hand, HLA-A and -B molecules are down-regulated in HIV-1-infected cell mostly due to the effect of Nef whereas HLA-C molecules are not, implying that HLA-C-restricted HIV-specific CTL can be elicited and have some role in the control of HIV-1. A previous study demonstrated that HLA-C-restricted responses are elicited in an African cohort infected with HIV-1 clade C, although it showed that HLA-B-restricted T-cell responses are much stronger than those of HLA-C-restricted or HLA-A-restricted ones [38]. A study using HLA-C-restricted HIV-1-specific CTL clones previously demonstrated that the ability of HLA-C-restricted CTL to suppress HIV-1 replication *in vitro* is similar

to that of HLA-A- or HLA-B-restricted CTL [28]. The present study also demonstrated that two HLA-C-restricted CTL had a strong ability to suppress HIV-1 replication *in vitro*. These findings suggested the possibility that some HLA-C-restricted T cells can control HIV-1 *in vivo*.

Previous studies demonstrated that HLA-A-restricted or HLA-B-restricted HIV-1-specific CTL recognised target cells infected with NL-432 M20A mutant (one amino acid substitution of Ala for Met at residue 20 of Nef), which lost the ability to down-regulate HLA-A and HLA-B molecules in HIV-1-infected cells, much more than those infected with NL-432 [12, 35, 39]. For example, Gag263-10-specific and Rev77-9-specific CTL showed approximately 50% suppression of the M20A virus replication but did not suppress NL432 replication (Supporting Information Table 1). Thus, HLA-C-restricted CTL, which is not affected by the Nef-mediated HLA down-regulation, have an advantage in the recognition of HLA–epitope complex on HIV-1-infected cells *in vivo*.

Previous population studies analysing HIV sequences in African cohorts demonstrated that some amino acid substitutions of HIV-1 Gag, Pol, and Nef are associated with HLA-C alleles [32, 33]. These studies suggested possibility that these substitutions are escape mutations selected by HLA-C-restricted T cells. However, since they did not demonstrate that specific CTL failed to recognise these substitutions, it still remained unclear whether HLA-C-restricted T cells could select escape mutant. We demonstrated here that the Pol463-10-specific CTL failed to kill the 9A mutant-infected cells but effectively killed WT HIV-1-infected ones. In addition, the CTL had a strong ability to suppress replication of a WT of HIV-1 but no ability to suppress that of the 9A mutant. The longitudinal analysis of HLA-Cw*1202$^+$ HIV-1-infected individuals showed the mutation from the WT to the 9A mutant. These results together support the idea that HLA-C-restricted CTL selected this escape mutant *in vivo*.

A previous study on a cohort infected with HIV-1 clade C virus demonstrated that HLA-C allele-associated Pol mutations are associated with low VL [33], suggesting these mutations increase fitness cost. The present study also demonstrated that NL-432 carrying the 9A mutant had a higher fitness cost than NL-432. However, the analysis of HLA-Cw*1202$^+$ individuals having and not having this mutation showed no association between VL and the presence of this mutation (data not shown). These suggest the possibility that a complementary substitution may compensate the effect of the 9A in terms of fitness cost. Another explanation is that fitness cost of the 9A mutant virus is not so much higher than that of the WT virus *in vivo*. Indeed, the difference in fitness cost between the two viruses in primary CD4$^+$ T cells is much smaller than that between them in the cell lines.

Both Pol 328-9-specific and Pol 463-10-specific CTL had strong ability to suppress HIV replication *in vitro*. However, the latter CTL selected escape mutants whereas the former CTL did not. It remains unknown why the one could select an escape mutant but the other could not. A recent study demonstrated that HLA-A*1101-restricted Nef73-specific and Nef84-specific CTL clones have strong ability to suppress HIV-1 replication *in vitro* but that the latter CTL can select an escape mutant whereas the former one did not [37]. *Ex vivo* analysis of these CTL showed that Nef84-specific CTL have a stronger ability to recognise the epitope than the Nef73-specific CTL [37]. That study suggested that only CTL having a strong ability to recognise the epitope can suppress HIV-1 replication *in vivo* so that escape mutants may be selected. This might be the case also for these HLA-Cw*1202-restricted CTL.

A variant 35 kb upstream of the *HLA-C* gene (*−35C/T*) was previously shown to be associated with the HLA-C mRNA expression level and steady-state plasma HIV RNA levels [29]. A recent study analysing 1698 European American individuals demonstrated that the *−35CC* allele is a proxy for high cell surface expression of HLA-C and that individuals with this allele progress more slowly to AIDS and control viremia significantly better than those without this low allele [40]. HLA-Cw*1202 is frequently found in east-Asia including Japan and forms a haplotype with HLA-A*2402 and HLA-B*5201. HLA-Cw*1202 is known to be highly associated with *−35CC* allele [40]. Therefore, we speculate that HLA-Cw*1202 is associated with a slow progression to AIDS.

In the present study, we demonstrated that HLA-Cw*1202-restricted Pol 463-10-specific CTL, which had a strong ability to suppress HIV-1 replication, selected an escape mutant, indicating that HLA-C allele-restricted HIV-specific CTL also play an important role in the generation of HIV-1 polymorphism. Further analysis of HLA-C-restricted CTL is expected to clarify the role of HLA-C alleles in HIV-1 infections.

Materials and methods

Samples of HIV-1-infected individuals

Plasma and PBMC were separated from whole blood of chronically HIV-1-infected individuals. The National Center for Global Health and Medicine and the Kumamoto University Ethical Committee approved this study. Informed consent was obtained from all subjects according to the Declaration of Helsinki.

HLA-typing

The HLA type of the chronically HIV-1-infected individuals was determined by standard sequence-based genotyping.

Synthetic peptides

We previously designed and generated overlapping peptides consisting of 11-mer or 17-mer amino acids in length and spanning Gag, Pol, and Nef of HIV-1 clade B consensus sequences [41, 42]. Each 11-mer and 17-mer peptide was overlapped by at least 9 and 11 amino acids, respectively.

Sequence of autologous virus

Viral RNA was extracted from plasma samples from HIV-1-infected individuals using a QIAamp MinElute virus spin kit (QIAGEN). cDNA was synthesised from the viral RNA using Cloned AMV First-Strand cDNA Synthesis kit (Invitrogen). The Pol regions including the two epitopes was amplified by nested PCR, and amplified products were used for sequencing reaction by BigDye Terminator v1.1 Cycle Sequencing kit (Applied Biosystems). DNA sequencing was performed by ABI PRISM 310 Genetic Analyzer (Applied Biosystems).

Cells

The EBV-transformed B-LCL were generated by transforming B cells from PBMC of healthy volunteers and HIV-1-seropositive individuals, KI-069, and KI-108. C1R cells expressing HLA-Cw*1202 (C1R-HLA-Cw*1202) were generated by transfecting C1R cells with the HLA-Cw*1202 gene; 721.221-CD4-HLA-Cw*1202 cells were generated by transfecting 721.221-CD4 cells with HLA-Cw*1202 genes. These transfectants were cultured in RPMI 1640 supplemented with 10% FBS and 0.15/mL hygromycin B. H9 cells were cultured in RPMI 1640 supplemented with 10% FBS. MGIC-5 cells (CCR5-transduced HeLa-CD4/LTR-β-gal cells) were cultured in DMEM supplemented with 10% FBS as described previously [43].

Generation of 2 HLA-Cw*1202-restricted HIV-1-specific CTL clones

The two Pol-epitope-specific CTL clones were generated from bulk CTL specific for Pol328-9 or Pol463-10 epitopes as described previously [37].

Generation of NL–432–$_{Pol\,463–10–9A}$ mutant clones

The NL-432-$_{Pol\ 463\text{-}10\text{-}9A}$ mutant virus was generated by introducing the Pol463-10-9A mutation into NL-432 using site-directed mutagenesis (Invitrogen).

Intracellular cytokine assay

PBMC from HLA-Cw*1202-positive HIV-1-infected patients were stimulated with HIV-1-derived peptide (1 μM) in culture medium (RPMI 1640 medium supplemented with 10% FBS and 200 U/mL recombinant human IL-2). After 14 days in culture, the cells were assessed for IFN-γ production using a FACS Calibur (BD Bioscience). Briefly, bulk cultures were stimulated with HLA-Cw*1202-expressing cells pulsed with HIV-1-derived peptide (1 μM) for 2 h at 37°C. Brefeldin A (10 μg/mL) was added, and incubated for a further 4 h. The cells were collected and stained with PE-labelled anti-CD8 mAb (Dako, Glostrup, Denmark). Cells were fixed with 4% paraformaldehyde solution, and permeabilised with permeabilization buffer (0.1% saponin and 20% Newborn Calf Serum in PBS) at 4°C for 10 min, followed by staining with FITC-labelled anti-IFN-γ mAb (PharMingen, San Diego, CA).

CTL assay for target cells pulsed with HIV-1 peptide

Cytotoxic activity of HIV-1-specific CTL was measured by the standard ^{51}Cr release assay, as previously described [12]. Briefly, target cells were labelled by $Na_2^{51}CrO_4$, then washed three times with RPMI 1640-10% FBS. ^{51}Cr-labelled target cells were plated 96-U plate with or without 1 μM peptide, and incubated for 1 h. After 1 h of incubation, CTL clones were added and incubated for 4 h. The supernatants were harvested and measured by a γ counter.

CTL assay for target cells infected with HIV-1

721.221-CD4-HLA-Cw*1202 cells were exposed to NL-432 or NL-432-$_{Pol\ 463\text{-}10\text{-}9A}$ for 3–6 days. Infection rate of these cells were measured by staining HIV-1 p24 Ag (KC57-FITC; Beckman Coulter). When approximately 30–60% of cells were infected, ^{51}Cr-labeled infected cells were co-cultured with CTL clones for 6 h. The supernatants were harvested and measured by a γ counter.

Replication suppression assay

The ability of HIV-1-specific CTL to suppress HIV-1 replication was examined as previously described [41]. Briefly, $CD4^+$ T cells were incubated with a given HIV-1 clone for 6 h at 37°C. After three washes with RPMI 1640-10% FBS, the cells were co-cultured with HIV-1-specific CTL clones. From day 3 to day 9 post infection, 10 μL of culture supernatant was collected; and the concentration of p24 Ag in it was measured with an enzyme immunoassay (HIV-1 p24 Ag ELISA kit; ZeptoMetrix, Buffalo, NY). The percentage of suppression of HIV-1 replication was calculated as follows: % suppression = (1–concentration of p24 Ag in the supernatant of HIV-1-infected $CD4^+$ T cells cultured with HIV-1-specific CTL/concentration of p24 Ag in the supernatant of HIV-1-infected $CD4^+$ T cells cultured without the CTL) × 100.

p24 production assay

H9 cells (8×10^5) and $CD4^+$ T cells (8×10^5) were exposed to each infectious virus preparation (500 blue cell-forming units in MAGIC-5 cells) for 6 h, washed twice with PBS, and cultured in 5 mL of complete medium [43]. The culture supernatants (0.2 mL) were harvested every other day, and the volume removed was replaced with fresh medium. The concentration of p24 Ag was measured with of an enzyme immunoassay (HIV-1 p24 Ag ELISA kit; ZeptoMetrix). Replication kinetics assays were performed in duplicate.

Competitive HIV-1 replication assay

Freshly prepared H9 cells (3×10^5) and $CD4^+$ T cells (3×10^5) were exposed for 2 h to mixtures of paired virus preparations (various blue cell-forming units) for examination of their replication ability, washed twice with PBS, and cultured as described previously [43]. Every other day the supernatant was harvested, and then cDNA was synthesised and sequenced. The change in viral population was determined from the relative peak height on sequencing electrograms.

ELISPOT assay

ELISPOT assay was performed as previously described [37]. Briefly, cryopreserved PBMC of 25 HLA-Cw^*1202^+ HIV-1-infected individuals were plated in 96-well polyvinylidene plates precoated with 0.5 μg/mL of anti-IFN-γ mAb 1-DIK (Matbech, Stockholm, Sweden). The appropriate amount of Pol 328-9 or Pol 463-10 peptide and PBMC were added at 1×10^5 cells/well and then the plates were incubated for 40 h. After the addition of biotinylated anti-IFN-γ mAb at 0.5 μg/mL, plates were incubated at room temperataure for 100 min. and then washed with PBS. Subsequently, streptavidin-conjugated alkaline phospatase was added, followed by 40 min incubation at room temperature. Individual cytokine-producing cells were detected as dark spots after a 20-min reaction with 5-bromo-4-chloro-3-indolyl phosphate and nitro blue tetrazolium using an alkaline phosphatase-conjugate substrate (Bio-Rad, Richmond, CA).

Acknowledgements: The authors thank Sachiko Sakai for her secretarial assistance. This research was supported by the Program of Founding Research Centers for Emerging and Reemerging Infectious Diseases and by the Global COE program [Global Education and Research Center Aiming at the control of AIDS,] launched as a project commissioned by the Ministry of Education, Science, Sports, and Culture, Japan; by a grant-in-aid for scientific research from the Ministry of Health, Japan; by a grant-in-aid for scientific research from the Ministry of Education, Science, Sports and Culture (No. 18390141, No. 20390134), Japan.

Conflict of interest: The authors declare no financial or commercial conflict of interest.

References

1 Ogg, G. S., Jin, X., Bonhoeffer, S., Dunbar, P. R., Nowak, M. A., Monard, S., Segal, J. P. *et al.*, Quantitation of HIV-1-specific cytotoxic T lymphocytes and plasma load of viral RNA. *Science* 1998. 279: 2103–2106.

2 Goulder, P. J. and Watkins, D. I., Impact of MHC class I diversity on immune control of immunodeficiency virus replication. *Nat. Rev. Immunol.* 2008. 8: 619–630.

3 Kawashima, Y., Kuse, N., Gatanaga, H., Naruto, T., Fujiwara, M., Dohki, S., Akahoshi, T. *et al.*, Long-term control of HIV-1 in hemophiliacs carrying slow-progressing allele HLA-B*5101. *J. Virol.* 2010. 84: 7151–7160.

4 Borrow, P., Lewicki, H., Wei, X., Horwitz, M. S., Peffer, N., Meyers, H., Nelson, J. A. *et al.*, Antiviral pressure exerted by HIV-1-specific cytotoxic T lymphocytes (CTLs) during primary infection demonstrated by rapid selection of CTL escape virus. *Nat. Med.* 1997. 3: 205–211.

5 Koup, R. A., Safrit, J. T., Cao, Y., Andrews, C. A., McLeod, G., Borkowsky, W., Farthing, C. *et al.*, Temporal association of cellular immune responses with the initial control of viremia in primary human immunodeficiency virus type 1 syndrome. *J. Virol.* 1994. 68: 4650–4655.

6 Harrer, E., Harrer, T., Buchbinder, S., Mann, D. L., Feinberg, M., Yilma, T., Johnson, R. P. *et al.*, HIV-1-specific cytotoxic T lymphocyte response in healthy, long-term nonprogressing seropositive persons. *AIDS Res. Hum. Retroviruses* 1994. 10: S77–S78.

7 Rinaldo, C., Huang, X. L., Fan, Z. F., Ding, M., Beltz, L., Logar, A., Panicali, D. *et al.*, High levels of anti-human immunodeficiency virus type 1 (HIV-1) memory cytotoxic T-lymphocyte activity and low viral load are associated with lack of disease in HIV-1-infected long-term nonprogressors. *J. Virol.* 1995. 69: 5838–5842.

8 Gandhi, R. T. and Walker, B. D., Immunologic control of HIV-1. *Annu. Rev. Med.* 2002. 53: 149–172.

9 Goulder, P. J., Phillips, R. E., Colbert, R. A., McAdam, S., Ogg, G., Nowak, M. A., Giangrande, P. *et al.*, Late escape from an immunodominant cytotoxic T-lymphocyte response associated with progression to AIDS. *Nat. Med.* 1997. 3: 212–217.

10 Price, D. A., Goulder, P. J., Klenerman, P., Sewell, A. K., Easterbrook, P. J., Troop, M., Bangham, C. R. *et al.*, Positive selection of HIV-1 cytotoxic T lymphocyte escape variants during primary infection. *Proc. Natl. Acad. Sci. USA* 1997. 94: 1890–1895.

11 Kelleher, A. D., Long, C., Holmes, E. C., Allen, R. L., Wilson, J., Conlon, C., Workman, C. *et al.*, Clustered mutations in HIV-1 gag are consistently required for escape from HLA-B27-restricted cytotoxic T lymphocyte responses. *J. Exp. Med.* 2001. 193: 375–386.

12 Fujiwara, M., Tanuma, J., Koizumi, H., Kawashima, Y., Honda, K., Mastuoka-Aizawa, S., Dohki, S. *et al.*, Different abilities of escape mutant-specific cytotoxic T cells to suppress replication of escape mutant and wild-type human immunodeficiency virus type 1 in new hosts. *J. Virol.* 2008. 82: 138–147.

13 Cohen, G. B., Gandhi, R. T., Davis, D. M., Mandelboim, O., Chen, B. K., Strominger, J. L. and Baltimore, D., The selective downregulation of class I major histocompatibility complex proteins by HIV-1 protects HIV-infected cells from NK cells. *Immunity* 1999. 10: 661–671.

14 Williams, M., Roeth, J. F., Kasper, M. R., Fleis, R. I., Przybycin, C. G. and Collins, K. L., Direct binding of human immunodeficiency virus type 1 Nef to the major histocompatibility complex class I (MHC-I) cytoplasmic tail disrupts MHC-I trafficking. *J. Virol.* 2002. 76: 12173–12184.

15 Arien, K. K. and Verhasselt, B., HIV Nef: role in pathogenesis and viral fitness. *Curr. HIV Res.* 2008. 6: 200–208.

16 Lama, J., The physiological relevance of CD4 receptor down-modulation during HIV infection. *Curr. HIV Res.* 2003. 1: 167–184.

17 Chowers, M. Y., Spina, C. A., Kwoh, T. J., Fitch, N. J., Richman, D. D. and Guatelli, J. C., Optimal infectivity *in vitro* of human immunodeficiency virus type 1 requires an intact nef gene. *J. Virol.* 1994. 68: 2906–2914.

18 Couillin, I., Connan, F., Culmann-Penciolelli, B., Gomard, E., Guillet, J. G. and Choppin, J., HLA-dependent variations in human immunodeficiency virus Nef protein alter peptide/HLA binding. *Eur. J. Immunol.* 1995. 25: 728–732.

19 Hashimoto, M., Kitano, M., Honda, K., Koizumi, H., Dohki, S., Oka, S. and Takiguchi, M., Selection of escape mutation by Pol154-162-specific cytotoxic T cells among chronically HIV-1-infected HLA-B*5401-positive individuals. *Hum. Immunol.* 2010. 71: 123–127.

20 Allen, T. M., O'Connor, D. H., Jing, P., Dzuris, J. L., Mothe, B. R., Vogel, T. U., Dunphy, E. *et al.*, Tat-specific cytotoxic T lymphocytes select for SIV escape variants during resolution of primary viraemia. *Nature* 2000. 407: 386–390.

21 Evans, D. T., O'Connor, D. H., Jing, P., Dzuris, J. L., Sidney, J., da Silva, J., Allen, T. M. *et al.*, Virus-specific cytotoxic T-lymphocyte responses select for amino-acid variation in simian immunodeficiency virus Env and Nef. *Nat. Med.* 1999. 5: 1270–1276.

22 McMichael, A. J. and Rowland-Jones, S. L., Cellular immune responses to HIV. *Nature* 2001. 410: 980–987.

23 Barouch, D. H., Kunstman, J., Kuroda, M. J., Schmitz, J. E., Santra, S., Peyerl, F. W., Krivulka, G. R. *et al.*, Eventual AIDS vaccine failure in a rhesus monkey by viral escape from cytotoxic T lymphocytes. *Nature* 2002. 415: 335–339.

24 Feeney, M. E., Tang, Y., Roosevelt, K. A., Leslie, A. J., McIntosh, K., Karthas, N., Walker, B. D. *et al.*, Immune escape precedes breakthrough human immunodeficiency virus type 1 viremia and broadening of the cytotoxic T-lymphocyte response in an HLA-B27-positive long-term-nonprogressing child. *J. Virol.* 2004. 78: 8927–8930.

25 Kawashima, Y., Pfafferott, K., Frater, J., Matthews, P., Payne, R., Addo, M., Gatanaga, H. *et al.*, Adaptation of HIV-1 to human leukocyte antigen class I. *Nature* 2009. 458: 641–645.

26 Neisig, A., Melief, C. J. and Neefjes, J., Reduced cell surface expression of HLA-C molecules correlates with restricted peptide binding and stable TAP interaction. *J. Immunol.* 1998. 160: 171–179.

27 McCutcheon, J. A., Gumperz, J., Smith, K. D., Lutz, C. T. and Parham, P., Low HLA-C expression at cell surfaces correlates with increased turnover of heavy chain mRNA. *J. Exp. Med.* 1995. 181: 2085–2095.

28 Adnan, S., Balamurugan, A., Trocha, A., Bennett, M. S., Ng, H. L., Ali, A., Brander, C. *et al.*, Nef interference with HIV-1-specific CTL antiviral activity is epitope specific. *Blood* 2006. 108: 3414–3419.

29 Fellay, J., Shianna, K. V., Ge, D., Colombo, S., Ledergerber, B., Weale, M., Zhang, K. *et al.*, A whole-genome association study of major determinants for host control of HIV-1. *Science* 2007. 317: 944–947.

30 van Manen, D., Kootstra, N. A., Boeser-Nunnink, B., Handulle, M. A., van't Wout, A. B. and Schuitemaker, H., Association of HLA-C and HCP5 gene regions with the clinical course of HIV-1 infection. *AIDS* 2009. 23: 19–28.

31 Makadzange, A. T., Gillespie, G., Dong, T., Kiama, P., Bwayo, J., Kimani, J., Plummer, F. *et al.*, Characterization of an HLA-C restricted CTL response in chronic HIV infection. *Eur. J. Immunol.* 2010. 40:1036–1041.

32 Rousseau, C. M., Daniels, M. G., Carlson, J. M., Kadie, C., Crawford, H., Prendergast, A., Matthews, P. *et al.*, HLA class I-driven evolution of human immunodeficiency virus type 1 subtype c proteome: immune escape and viral load. *J. Virol.* 2008. 82: 6434–6446.

33 Matthews, P. C., Prendergast, A., Leslie, A., Crawford, H., Payne, R., Rousseau, C., Rolland, M. *et al.*, Central role of reverting mutations in HLA associations with human immunodeficiency virus set point. *J. Virol.* 2008. 82: 8548–8559.

34 De Groot, A. S., Jesdale, B., Martin, W., Saint Aubin, C., Sbai, H., Bosma, A., Lieberman, J. *et al.*, Mapping cross-clade HIV-1 vaccine epitopes using a bioinformatics approach. *Vaccine* 2003. 21: 4486–4504.

35 Tomiyama, H., Fujiwara, M., Oka, S. and Takiguchi, M., Cutting edge: epitope-dependent effect of Nef-mediated HLA class I down-regulation on ability of HIV-1-specific CTLs to suppress HIV-1 replication. *J. Immunol.* 2005. 174: 36–40.

36 Tomiyama, H., Akari, H., Adachi, A. and Takiguchi, M., Different effects of Nef-mediated HLA class I down-regulation on human immunodeficiency virus type 1-specific CD8(+) T-cell cytolytic activity and cytokine production. *J. Virol.* 2002. 76: 7535–7543.

37 Koizumi, H., Hashimoto, M., Fujiwara, M., Murakoshi, H., Chikata, T., Borghan, M. A., Hachiya, A. *et al.*, Different *in vivo* effects of HIV-1 immunodominant epitope-specific cytotoxic T lymphocytes on selection of escape mutant viruses. *J. Virol.* 2010. 84: 5508–5519.

38 Kiepiela, P., Leslie, A. J., Honeyborne, I., Ramduth, D., Thobakgale, C., Chetty, S., Rathnavalu, P. *et al.*, Dominant influence of HLA-B in mediating the potential co-evolution of HIV and HLA. *Nature* 2004. 432: 769–775.

39 Akari, H., Arold, S., Fukumori, T., Okazaki, T., Strebel, K. and Adachi, A., Nef-induced major histocompatibility complex class I down-regulation is functionally dissociated from its virion incorporation, enhancement of viral infectivity, and CD4 down-regulation. *J. Virol.* 2000. 74: 2907–2912.

40 Thomas, R., Apps, R., Qi, Y., Gao, X., Male, V., O'HUigin, C., O'Connor, G. *et al.*, HLA-C cell surface expression and control of HIV/AIDS correlate with a variant upstream of HLA-C. *Nat. Genet.* 2009. 41: 1290–1294.

41 Kitano, M., Kobayashi, N., Kawashima, Y., Akahoshi, T., Nokihara, K., Oka, S. and Takighuchi, M., Identification and characterization of HLA-B*5401-restricted HIV-1-Nef and Pol-specific CTL epitopes. *Microbes Infect.* 2008. 10: 764–772.

42 Zheng, N., Fujiwara, M., Ueno, T., Oka, S. and Takiguchi, M., Strong ability of Nef-specific CD4+cytotoxic T cells to suppress human immunodeficiency virus type 1 (HIV-1) replication in HIV-1-infected CD4+T cells and macrophages. *J. Virol.* 2009. 83: 7668–7677.

43 Gatanaga, H., Hachiya, A., Kimura, S. and Oka, S., Mutations other than 103N in human immunodeficiency virus type 1 reverse transcriptase (RT) emerge from K103R polymorphism under non-nucleoside RT inhibitor pressure. *Virology* 2006. 344: 354–362.

Abbreviations: **B-LCL:** B-lymphoblastoid cell lines · **V9A:** V-to-A substitution at the 9th position · **VL:** viral load

Full correspondence: Prof. Masafumi Takiguchi, Center for AIDS Research, Kumamoto University, 2-2-1 Honjo, Kumamoto 860-0811, Japan
Fax: +81-96-373-6532
e-mail: masafumi@kumamoto-u.ac.jp

Received: 16/7/2010
Revised: 22/9/2010
Accepted: 22/10/2010
Accepted article online: 19/11/2010

K70Q Adds High-Level Tenofovir Resistance to "Q151M Complex" HIV Reverse Transcriptase through the Enhanced Discrimination Mechanism

Atsuko Hachiya[1,2], Eiichi N. Kodama[3]*, Matthew M. Schuckmann[1], Karen A. Kirby[1], Eleftherios Michailidis[1], Yasuko Sakagami[4], Shinichi Oka[2], Kamalendra Singh[1], Stefan G. Sarafianos[1]*

1 Department of Molecular Microbiology and Immunology, University of Missouri School of Medicine, Columbia, Missouri, United States of America, **2** AIDS Clinical Center, National Center for Global Health and Medicine, Tokyo, Japan, **3** Division of Emerging Infectious Diseases, Tohoku University School of Medicine, Sendai, Japan, **4** Institute for Virus Research, Kyoto University, Kyoto, Japan

Abstract

HIV-1 carrying the "Q151M complex" reverse transcriptase (RT) mutations (A62V/V75I/F77L/F116Y/Q151M, or Q151Mc) is resistant to many FDA-approved nucleoside RT inhibitors (NRTIs), but has been considered susceptible to tenofovir disoproxil fumarate (TFV-DF or TDF). We have isolated from a TFV-DF-treated HIV patient a Q151Mc-containing clinical isolate with high phenotypic resistance to TFV-DF. Analysis of the genotypic and phenotypic testing over the course of this patient's therapy lead us to hypothesize that TFV-DF resistance emerged upon appearance of the previously unreported K70Q mutation in the Q151Mc background. Virological analysis showed that HIV with only K70Q was not significantly resistant to TFV-DF. However, addition of K70Q to the Q151Mc background significantly enhanced resistance to several approved NRTIs, and also resulted in high-level (10-fold) resistance to TFV-DF. Biochemical experiments established that the increased resistance to tenofovir is not the result of enhanced excision, as K70Q/Q151Mc RT exhibited diminished, rather than enhanced ATP-based primer unblocking activity. Pre-steady state kinetic analysis of the recombinant enzymes demonstrated that addition of the K70Q mutation selectively decreases the binding of tenofovir-diphosphate (TFV-DP), resulting in reduced incorporation of TFV into the nascent DNA chain. Molecular dynamics simulations suggest that changes in the hydrogen bonding pattern in the polymerase active site of K70Q/Q151Mc RT may contribute to the observed changes in binding and incorporation of TFV-DP. The novel pattern of TFV-resistance may help adjust therapeutic strategies for NRTI-experienced patients with multi-drug resistant (MDR) mutations.

Citation: Hachiya A, Kodama EN, Schuckmann MM, Kirby KA, Michailidis E, et al. (2011) K70Q Adds High-Level Tenofovir Resistance to "Q151M Complex" HIV Reverse Transcriptase through the Enhanced Discrimination Mechanism. PLoS ONE 6(1): e16242. doi:10.1371/journal.pone.0016242

Editor: Zandrea Ambrose, University of Pittsburgh, United States of America

Received September 15, 2010; **Accepted** December 8, 2010; **Published** January 13, 2011

Funding: This work was supported by a grant for the promotion of AIDS Research from the Ministry of Health, Labor and Welfare (AH and EK, http://www.mhlw.go.jp/english/index.html), by grants from the Korea Food & Drug Administration and the Ministry of Knowledge and Economy, Bilateral International Collaborative R&D Program, Republic of Korea (SGS) and by National Institutes of Health (NIH, http://nih.gov/) research grants AI094715, AI076119, AI079801, and AI074389 to SGS. The funders had no role in study design, data collection and analysis, decision to publish, or preparation of the manuscript.

Competing Interests: The authors have declared that no competing interests exist.

* E-mail: sarafianoss@missouri.edu (SGS); kodama515@m.tains.tohoku.ac.jp (ENK)

Introduction

Nucleos(t)ide reverse transcriptase inhibitors (NRTIs) are used in combination with other classes of drugs for the treatment of patients infected with human immunodeficiency virus type-1 (HIV-1). This approach is known as highly active anti-retroviral therapy (HAART) and has been remarkably successful in reducing the viral loads and increasing the number of CD4+ cells in patients' plasma. However, prolonged therapies inevitably result in resistance to all of the available drugs. Several mutations in the reverse transcriptase (RT) are known to cause resistance to NRTIs through two basic mechanisms:

1) The excision mechanism, which is based on an enhanced capacity of RT to use adenosine triphosphate (ATP) as a nucleophile for the removal of the chain-terminating nucleotide from the DNA terminus. The excision reaction products are a 5′, 5′-dinucleoside tetraphosphate and an unblocked primer with a free 3′-OH, allowing DNA synthesis to resume [1,2,3]. Increased excision of NRTIs is imparted by Excision Enhancement Mutations, typically M41L, D67N, K70R, T215Y/F, L210W, and K219E/Q (also known as Thymidine Associated Mutations, or TAMs). Other mutations have also been reported to enhance excision, including insertions or deletions at the tip of the β3- β4 loop of the fingers subdomain in the background of other excision enhancement mutations [4,5,6,7,8,9,10,11].

2) The other mechanism of NRTI resistance is the exclusion mechanism, which is caused when NRTI-resistance mutations in RT enhance discrimination and reduce incorporation of the NRTI-triphosphate (NRTI-TP). This mechanism is exemplified by the resistance of the M184V RT mutant to lamivudine (3TC) and emtricitabine (FTC) due to steric clash between the β-branched Val or Ile at position 184 and the oxathiolane ring of the inhibitors [12,13]. Another example of the exclusion mechanism is the multi-drug resistant (MDR) HIV-1 RT known as Q151M complex (Q151Mc). This RT contains the Q151M mutation together with a cluster of four

additional mutations (A62V/V75I/F77L/F116Y) [14,15]. Q151M by itself causes intermediate- to high-level resistance to zidovudine (AZT), didanosine (ddI), zalcitabine (ddC), stavudine (d4T), and low level resistance to abacavir (ABC) [15,16,17] without reducing viral fitness [18,19]. Addition of the four associated mutations increases replication capacity of RT and results in high-level resistance to AZT, ddI, ddC, and d4T, 5-fold resistance to ABC and low-level resistance to lamivudine (3TC) and emtricitabine (FTC) [17,18,19,20,21]. Miller *et al.* and Smith *et al.* reported a 1.8-fold and 3.6-fold increase in resistance to tenofovir (TFV), respectively [22,23].

Biochemical studies on the mechanism of Q151Mc resistance to multiple NRTIs have revealed that the mutations of this complex decrease the maximum rate of NRTI-TP incorporation without significantly affecting the incorporation of the natural nucleotides [21,24,25]. Structurally, the Q151 residue interacts with the 3′-OH of a normal deoxynucleoside triphosphate (dNTP) substrate [26]. It appears that the Q151Mc mutations cause resistance to multiple NRTIs by affecting the hydrogen bond network involving protein side chains in the vicinity of the dNTP-binding site and the NRTI triphosphate lacking a 3′-OH [25,26,27]. The Q151Mc set of mutations was also reported to decrease pyrophosphate PPi- and ATP-mediated excision [25].

K65R is another mutation near the polymerase active site that confers NRTI resistance through the exclusion mechanism. Specifically, K65R RT has reduced susceptibility to the acyclic nucleotide analog, TFV and other NRTIs, including ddI, ddC, ABC, FTC and 3TC [28,29,30,31]. Biochemical studies with K65R RT have demonstrated that this enzyme decreases the incorporation rate of these NRTIs [32,33,34]. The crystal structure of K65R RT in complex with DNA and TFV diphosphate (TFV-DP) revealed that R65 forms a molecular platform with the conserved residue R72, and the platform enhances the ability of K65R RT to discriminate NRTIs from dNTPs [35]. HIV carrying the Q151Mc mutations has been reported to be susceptible to TFV disoproxil fumarate (TFV-DF), the oral prodrug of TFV that enhances its oral bioavailability and anti-HIV activity [22,36]. While the K65R mutation appeared in several patients treated for more than 18 months with TFV-DF, no patient developed multi-NRTI resistance through appearance of Q151Mc [37].

Here we report the identification of unique HIV clinical isolates that have acquired the K70Q mutation in the background of Q151Mc during TFV-DF-containing therapy. We have used a combination of virological, biochemical, and molecular modeling methods to derive the mechanism by which this mutation confers resistance to TFV.

Materials and Methods

Clinical samples

HIV was isolated from fresh plasma immediately after collection of clinical samples from study participants at the outpatient clinic of the AIDS Clinical Center (ACC), International Medical Center of Japan. The Institutional Review Board approved this study (IMCJ-H13-80) and a written consent was obtained from all participants.

Construction of recombinant clones of HIV-1

Recombinant infectious clones of HIV-1 carrying various mutations were prepared using standard site-directed mutagenesis protocols as described previously [38]. The NL4-3-based molecular clone was constructed by replacing the *pol*-coding region with the HIV-1 BH10 strain. Restriction enzyme sites *Xma I* and *Nhe I* were introduced by silent mutations into the molecular clone at positions corresponding to HIV-1 RT codons 15 and 267, respectively [39]. Each molecular clone was transfected into COS-7 cells. Cells were grown for 48 h, and culture supernatants were harvested and stored at −80°C until use.

Single-cycle drug susceptibility assay

Susceptibilities to various RT inhibitors were determined using the MAGIC-5 cells which are HeLa cells stably transfected with a β-galactosidase gene under the control of an HIV long terminal repeat promoter, and with vectors that express the CD4 receptor and the CCR5 co-receptor under the control of the CMV promoter as described previously [40]. Briefly, MAGIC-5 cells were infected with diluted virus stock (100 blue forming units) in the presence of increasing concentrations of RT inhibitors, cultured for 48 h, fixed, and stained with X-Gal (5-bromo-4-chloro-3-indolyl-β-D-galacto-pyranoside). The stained cells were counted under a light microscope. Drug concentrations reducing the number of infected cells to 50% of the drug-free control (EC_{50}) were determined from dose response curves.

Enzymes

RT sequences coding for the p66 and p51 subunits of BH10 were cloned in the pRT dual vector, which is derived from pCDF-2 with LIC duet minimal adaptor (Novagen), using restriction sites *PpuMI* and *SacI* for the p51 subunit, and *SacII* and *AvrII* for the p66 subunit. RT was expressed in the *Escherichia coli* strain BL21 (Invitrogen) and purified by nickel affinity chromatography and MonoQ anion exchange chromatography [41]. RT concentrations were determined spectrophotometrically based on absorption at 260 nm using a calculated extinction coefficient (261,610 M^{-1} cm^{-1}). The active site concentration of the various RT preparations was calculated as described below.

Nucleic acid substrates

DNA oligomers were synthesized by Integrated DNA Technologies (Coralville, IA). An 18-nucleotide DNA primer fluorescently labeled with Cy3 at the 5′ end (P_{18}; 5′-Cy3 GTC CCT GTT CGG GCG CCA-3′) and a 100-nucleotide DNA template (T_{100}; 5′-TAG TGT GTG CCC GTC TGT TGT GTG ACT CTG GTA ACT AGA GAT CCC TCA GAC CCT TTT AGT CAG TGT GGA AAA TCT CTA GCA GTG GCG CCC GAA CAG GGA C-3′) were used in primer extension assays. An 18-nucleotide DNA primer 5′-labeled with Cy3 (P_{18}; 5′-Cy3 GTC ACT GTT CGA GCA CCA-3′) and a 31-nucleotide DNA template (T_{31}; 5′- CCA TAG CTA GCA TTG GTG CTC GAA CAG TGA C-3′) were used in the ATP rescue assay and pre-steady state kinetic experiments.

Active site titration and determination of the dissociation constant for DNA binding ($K_{D\text{-}DNA}$)

Determination of active site concentrations in the different preparations of WT and mutant RTs were performed using pre-steady state burst experiments. A fixed concentration of RT (80 nM, determined by absorbance measurements) was pre-incubated with increasing concentrations of DNA/DNA template/primer (T_{31}/P_{18}), followed by rapidly mixing with a reaction mixture containing $MgCl_2$ and dATP, at final concentrations of 5 mM and 50 μM, respectively. The reactions were quenched at various times (10 ms to 5 s) by adding EDTA to a final concentration of 50 mM. The amounts of product (P_{18}-dAMP) were quantitated and fit to the following burst equation:

$$P = A\left(1 - e^{-kobst}\right) + k_{ss}t \quad (1)$$

where A is the amplitude of the burst phase that represents the RT-DNA complex at the start of the reaction, k_{obs} is the observed burst rate constant for dNTP incorporation, k_{ss} is the steady state rate constant, and t is the reaction time. The rate constant of the linear phase (k_{cat}) can be estimated by dividing the slope of the linear phase by the enzyme concentration. The active site concentration and template/primer binding affinity ($K_{D\text{-}DNA}$) were determined by plotting the amplitude (A) against the concentration of template/primer. The data were fit using non-linear regression to a quadratic equation:

$$A = 0.5(K_D + [RT] + [DNA]) - \sqrt{0.25(K_D + [RT] + [DNA])^2 - ([RT][DNA])} \quad (2)$$

where K_D is the dissociation constant for the RT-DNA complex, and [RT] is the concentration of active polymerase molecules. Subsequent biochemical experiments were performed using corrected active site concentrations [42,43].

Primer extension assay

To examine the DNA polymerase activity of WT and mutant RTs and the inhibition of DNA synthesis by TFV, the primer extension assays were carried out on the T_{100}/P_{18} template/primer (P_{18} was 5′-Cy3 labeled) in the presence or absence of 3.5 mM ATP [41]. The enzyme (20 nM active sites) was incubated with 20 nM template/primer at 37°C in a buffer containing 50 mM Tris-HCl, pH 7.8 and 50 mM NaCl. The DNA synthesis was initiated by the addition of 1 μM dNTP and 10 mM $MgCl_2$. The primer extension assays were carried out in the presence or absence of varying concentrations of TFV-DP. The reactions were terminated after 15 min by adding equal volume of 100% formamide containing traces of bromophenol blue. The extension products were resolved on a 7 M urea-15% polyacrylamide gel, and visualized by phosphor-imaging (FLA 5100, Fujifilm, Tokyo). We followed standard protocols that utilize the Multi Gauge software (Fujifilm) to quantitate primer extension [41,44]. The results from dose response experiments were plotted using Prism 4 (GraphPad Software Inc., CA) and IC_{50} values for TFV-DP were obtained at midpoint concentrations.

ATP-dependent rescue assay

Template/primer (T_{31}/P_{18}) terminated with TFV (T/P_{TFV}) was prepared as described in Michailidis et al [41]. 20 nM of T/P_{TFV} was incubated at 37°C with HIV-1 RT (60 nM), either at various concentrations of ATP (0–7 mM) for 30 minutes, or for various times (0–120 minutes) with 3.5 mM ATP, in RT buffer containing 50 mM Tris-HCl, pH 7.8, and 50 mM NaCl, and 10 mM $MgCl_2$. The assay was performed in the presence of excess competing dATP (100 μM) that prevented reincorporation of the excised TFV, 0.5 μM dTTP and 10 μM ddGTP. Reactions were quenched with 100% formamide containing traces of bromophenol blue and analyzed as described above. The dissociation constants (K_d) of the various enzymes for ATP used in the rescue reactions were determined by fitting the rescue data at various ATP concentrations, using non-linear regression fitting to hyperbola.

Kinetics of dNTP incorporation by WT and mutant enzymes

To determine the binding affinity of WT and mutant enzymes to the dNTP substrate ($K_{D\text{-}dNTP}$) and to estimate the maximum rate of dNTP incorporation by these enzymes (k_{pol}), we carried out transient-state experiments using a rapid quench instrument (RQF-3, Kintek Corporation, Clarence, PA) at 37°C in RT buffer (50 mM Tris-HCl, pH 7.8 and 50 mM NaCl). HIV-1 RT (50 nM active sites) was pre-incubated with 50 nM T_{31}/P_{18} in one syringe (Syringe A), whereas varying concentrations of dNTP and 10 mM $MgCl_2$ were kept in another syringe (Syringe B). The solutions were rapidly mixed to initiate reactions, which were subsequently quenched at various times (5 ms to 10 s) by adding EDTA to a final concentration of 50 mM. The products from each quenched reaction were resolved, quantitated, and plotted as described above. The data were fit by non-linear regression to the burst equation (Eq 1).

To obtain the dissociation constant $K_{D\text{-}dNTP}$ for dNTP binding to the RT-DNA complex, the observed burst rates (k_{obs}) were fit to the hyperbolic equation (Eq. 3) using nonlinear regression:

$$k_{obs} = \left(k_{pol}[dNTP]\right)/(K_{D-dNTP} + [dNTP]) \quad (3)$$

where k_{pol} is the optimal rate of dNTP incorporation.

The kinetics of TFV incorporation by the WT and mutant enzymes were carried out in a manner similar to that employed for natural dNTP substrate except the time of reactions. It was noted that the mutant enzymes required longer time to incorporate TFV compared to the WT HIV-1 RT (detailed in the Results section).

Molecular Modeling

Molecular models of mutant enzymes were generated using SYBYL (Tripos Associates, St. Louis, MO). The starting protein coordinates were from the crystal structure of HIV-1 RT in complex with DNA template/primer and TFV-DP (PDB file 1T05) [45]. They were initially modified by the Protein Preparation tool (Schrodinger Molecular Modeling Suit, NY), which deletes unwanted water molecules, sets charges and atom type of metal ions, corrects misoriented Gln and Asn residues, and optimizes H-atom orientations. Amino acid side chains were substituted in by Maestro (Schrodinger, Molecular Modeling Suite, NY). Molecular dynamics simulations of the WT and mutant RT models were carried out to obtain the most stable structures by Impact, interfaced with Maestro at constant temperature, and OPLS_2005 force field. The molecular dynamics simulations were performed for 1000 steps with 0.001 ps intervals. The temperature relaxation time was 0.01 ps. The Verlet integration algorithm was used in simulations. The structures were imported into Pymol (http://www.pymol.org) for visualization and comparison.

Results

Phenotypic resistance to TFV-DF in the absence of any known TFV resistance mutations

During phenotypic and genotypic evaluation of the clinical isolates we identified a unique virus that exhibited an apparent discordance between the phenotypic and genotypic results. The clinical history of the patient and the corresponding genotypic and phenotypic changes during the course of the therapy are summarized in Fig. 1. (Also see Table S1). The patient's treatment before Feb 2002 included d4T, ddI, and EFV and did not decrease significantly the viral loads (Fig 1A). Hence, the therapeutic regimen was switched to TFV-DF, EFV, and the protease inhibitor lopinavir (LPV). However, the patient's immunological and virological responses still did not improve due to poor adherence, especially to LPV. Genotypic and phenotypic analyses on March 2002 (point 1) and June 2002 (point 2) revealed

A

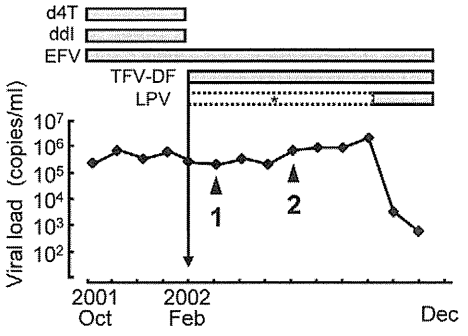

B Phenotypic profile

Isolate	Fold increase in EC_{50}								
	AZT	ddI	d4T	3TC	ABC	**TFV-DF**	FTC	NVP	EFV
1	61	12	9	13	10	**2**	9	>200	>500
2	57	>40	>50	31	15	**6**	5	>200	>500

C Genotypic profile

Isolate	Resistance-associated mutation		Other newly acquired mutations
	NRTI	NNRTI	
1	Q151M complex, V106M, V179D		-
2	Q151M complex, V106M, V179D, V108I	**K70Q**, K102R	

Figure 1. Clinical course of patient and drug resistance profile. (A) The two clinical isolates were collected from the patient at the time points indicated by triangles. Both isolates had no known resistant mutations in the protease region. During the period indicated by asterisk, LPV was administrated but the patient demonstrated poor adherence due to undesirable side effects. After instruction on the use of antiretroviral drugs, the viral loads successfully decreased below the detection limit (<50 copies/ml). (B) Phenotypic drug susceptibility assays of clinical isolates in at least three independent experiments are shown as a relative increase in EC_{50} compared to HIV-1 NL4-3 strain which served as WT (see also Table S1). (C) Mutations observed in the isolates that are defined as the NRTI and NNRTI resistance associated mutations deposited in the HIV Drug Resistance Database maintained by International AIDS Society 2009 [58] and the Stanford University (http://hivdb.stanford.edu/) were shown. Abbreviations of drugs used: d4T, stavudine; ddI, didenosine; EFV, efavirenz; TFV-DF, tenofovir disoproxil fumarate; LPV, lopinovir; AZT, zidovudine; 3TC, lamivudine; ABC, abacavir; FTC, emtricitabine; NVP, nevirapine.
doi:10.1371/journal.pone.0016242.g001

resistance to multiple RT inhibitors, including NNRTIs (Fig 1B). Resistance to all NRTIs, except AZT and FTC, was enhanced in the point 2 isolate (Fig. 1B). Notably, this isolate showed an increase in resistance to TFV-DF in the absence of the canonical TFV resistance mutation (K65R) and in the presence of Q151Mc mutations (Fig. 1C). Previously, it has been shown that Q151Mc remains susceptible to TFV [22] although Smith *et al.* reported that Q151Mc had a 3.6-fold increase in TFV resistance [23]. Suppression of the viral load was finally achieved by improvement in drug adherence to LPV and by the addition of FTC in the therapeutic regimen, since no protease resistance mutations were found within the protease coding region.

To identify the mutation(s) responsible for the unexpected resistance to TFV-DF we sequenced the entire RT coding region at time-points 1 and 2 (Figure S1, GenBank Accession Number AB506802 and AB506803). Of the three substituted residues (70, 102, and 108) amino acids 102 and 108 are part of the structurally distinct NNRTI binding pocket [46], which can mutate during EFV-based therapeutic regimens. However, residue 70 is located in the β3-β4 hairpin loop of the p66 "fingers" subdomain of HIV-1 RT, which interacts with the incoming dNTP substrate [10,27]. Different mutations at this site have been previously implicated in NRTI resistance [47], suggesting that the observed K70Q mutation may be involved in the increased resistance to TFV-DF.

NRTI resistance enhancement by mutation at residue 70

Several mutations at position 70 of HIV-1 RT (R, G, E, T, N and Q) have been reported to the Stanford HIV-1 Drug Resistance Database (http://hivdb.stanford.edu/, accessed on Feb. 27th 2010). K70Q is rarely observed in treatment-naïve patients (0.04%), but appears more often in clinical samples from NRTI-treated patients (0.1%, $p<0.0001$ compared with the frequency of K70Q in treatment-naïve patients) but not NNRTI-treated patients. Furthermore, K70Q is observed in 0.5% of the clinical samples from patients infected with HIV-1 Q151M. There have been no previous reports on a possible role of K70Q in NRTI resistance.

To examine the effect of K70Q on drug susceptibility we generated a series of HIV variants with mutations at RT codon 70 (Figure 2A and also Table S2). The HIV-1_{K70Q} variant exhibited marginal resistance to ddI and 3TC (5- and 3.3-fold, respectively), but no significant resistance to other NRTIs. We further examined whether the mutations at residue 70 affect susceptibility to NRTIs in the Q151Mc background (Figure 2B and also Table S3). HIV-$1_{K70G/Q151Mc}$ had enhanced resistance to d4T (4.6-fold) as compared to HIV-1_{Q151Mc}. Notably, HIV-$1_{K70Q/Q151Mc}$ also showed enhanced resistance to ddI and d4T (2.4- and 4.4-fold, respectively, compared to HIV-1_{Q151Mc}). In addition, HIV-$1_{K70Q/Q151Mc}$ displayed 5-fold increased resistance to TFV-DF compared to HIV-1_{Q151Mc}. Other K70 mutations exhibited little or no resistance to TFV-DF.

Primer Extension and ATP-based Rescue Assays

As mentioned earlier, a key mechanism of NRTI resistance is the excision mechanism, which is based on the enhanced ability of NRTI-resistant enzymes to use ATP for unblocking chain-terminated primers and allow for further DNA synthesis to continue [2,3,48]. To determine whether the K70Q mutation causes TFV resistance through the excision mechanism we measured the susceptibility of WT and mutant RTs to inhibition by TFV in the presence or absence of ATP. In gel-based assays, an enhancement in excision would manifest as an increase in the production of fully extended DNA when 3.5 mM ATP is included in the extension reaction [49,50]. Our extension assays in the absence of ATP (no-excision conditions) showed that addition of the K70Q mutation to Q151Mc HIV-1 RT enhances resistance to TFV-DP. However, this enhancement is not influenced by the presence of ATP (Table 1, Fig. 3A and Figure S2A). In fact, excision enhancement due to the presence of ATP measured as [IC_{50} with ATP]/[IC_{50} without ATP] was similar for all enzymes, including the WT RT (from 2.7-fold to 2.9-fold for WT, K70Q, Q151Mc, and K70Q/Q151Mc RTs) (Table 1). Using a related type of assay, the ATP-mediated rescue assay, we compared the rates by which the WT and mutant RTs unblock TFV-terminated primers and extend products past the point of chain-termination. We find that the ATP-based rescue activity of WT RT is not slower, but 1.5-, 2.5-, and 3-fold faster than that of K70Q, Q151Mc, and K70Q/Q151Mc RTs, respectively (Fig. 3B and Figure S2B). In addition, the ATP-based rescue activity of WT RT was saturated at lower concentrations of ATP than K70Q,

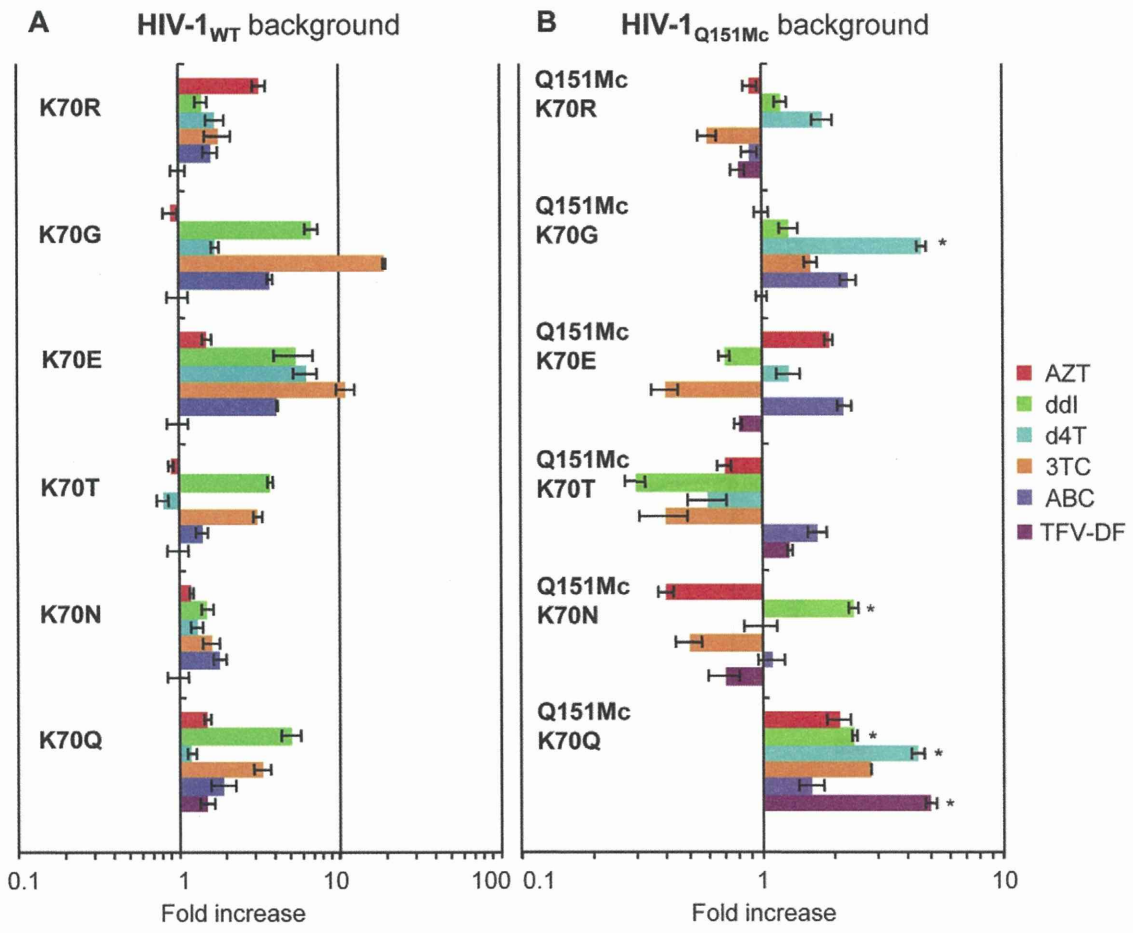

Figure 2. NRTI resistance of HIVs with mutations at RT residue 70 in the background of WT or Q151Mc. Antiviral activities of HIV-1s carrying mutations at residue 70 (K70R, K70G, K70E, K70T, K70N, or K70Q) in the WT (A) or Q151Mc (B) background were determined by the MAGIC5 assay. The data for each clone were compared to WT (A) and Q151Mc (B) HIV-1 and are shown as fold increase; AZT (red), ddI (green), d4T (cyan), 3TC (orange), ABC (blue), and TFV-DF (purple). Error bars represent standard deviations from at least three independent experiments (see also Table S2 and S3). The asterisk indicates statistically significant in EC_{50} values ($P<0.0001$ by t-test).
doi:10.1371/journal.pone.0016242.g002

Table 1. Primer extension assay in the presence or absence of ATP.

Enzyme[a]	IC_{50} (nM) of TFV-DP[b] (fold increase[c])		Excision enhancement due to ATP[d]
	Without ATP	**With ATP**	
WT	641±83	1854±197	2.9
	(1)[b]	(1)[b]	
K70Q	802±99	2306±270	2.9
	(1.3)	(1.2)	
Q151Mc	1503±90	3996±341	2.7
	(2.3)	(2.1)	
K70Q/Q151Mc	2392±353	7001±226	2.9
	(3.7)	**(3.8)**	

[a]The sequence of HIV RT WT and mutant derived from BH10.
[b]Data are means ± standard deviations from at least three independent experiments.
[c]The relative increase in IC_{50} value compared with each HIV-1 RT WT without, or with ATP is given in parentheses. Bold indicates an increase in fold increase value greater than 3-fold.
[d]Excision enhancement due to ATP is calculated as IC_{50} with ATP/IC_{50} without ATP.
doi:10.1371/journal.pone.0016242.t001